NRC Research Press

ARTICLE

Up, down, or sideways: emplacement of magmatic Fe–Ni–Cu–PGE sulfide melts in large igneous provinces[1]

C.M. Lesher

Abstract: The preferential localization of Fe–Ni–Cu–PGE sulfides within the horizontal components of dike–sill–lava flow complexes in large igneous provinces (LIPs) indicates that they were fluid dynamic traps for sulfide melts. Many authors have interpreted them to have collected sulfide droplets transported upwards, often from deeper "staging chambers". Although fine (<1–2 cm) dilute (<10%–15%) suspensions of dense (~4–5 g/cm^3) sulfide melt can be transported in ascending magmas, there are several problems with upward-transport models for almost all LIP-related deposits: (1) S isotopic data are consistent with nearby crustal sources, (2) xenoliths appear to be derived from nearby rather than deeper crustal sources, (3) lateral sheet flow or sill facies of major deposits contain few if any sulfides, (4) except where there is evidence for a local S source, sulfides or chalcophile element enrichments rarely if ever occur in the volcanic components even where there is mineralization in the subvolcanic plumbing system, and (5) some lavas are mildly to strongly depleted in PGE >>> Cu > Ni > Co, indicating that unerupted sulfides sequestered PGEs at depth. Two potential solutions to this paradox are that (*i*) natural systems contained surfactants that lowered sulfide–silicate interfacial tensions, permitting sulfide melts to coalesce and settle more easily than predicted from theoretical/experimental studies of artificial/analog systems, and (or) (*ii*) sulfides existed not as uniformly dispersed droplets, as normally assumed, but as fluid-dynamically coherent pseudoslugs or pseudolayers that were large and dense enough that they could not be transported upwards. Regardless of the ultimate explanation, it seems likely that most high-grade Ni–Cu–PGE sulfide deposits in LIPs formed at or above the same stratigraphic levels as they are found.

Key words: Ni–Cu–PGE deposits, magmatic sulfides, large igneous provinces.

Résumé : L'emplacement préférentiel de sulfures à Fe–Ni–Cu–EGP dans les composantes horizontales de complexes de dykes, filons-couches et coulées de lave dans de grandes provinces ignées (GPI) indique que ces composantes constituaient des pièges à l'écoulement de bains sulfurés. De nombreux auteurs les ont interprétées comme ayant été le lieu de collecte de gouttelettes de sulfures transportées vers le haut, souvent en provenance de « chambres d'escale ». Bien que de fines (<1–2 cm) suspensions diluées (<10 %–15 %) d'un bain sulfuré dense (~4–5 g/cm^3) puissent être transportées dans des magmas ascendants, les modèles de transport ascendant pour presque tous les gisements associés à des GPI posent plusieurs problèmes, à savoir : (1) les données sur les isotopes du S concordent avec des sources crustales proximales, (2) les xénolites semblent être dérivés de sources crustales proximales plutôt que de sources crustales plus profondes, (3) les faciès à coulées latérales ou à filons-couches de gisements importants ne contiennent peu ou pas de sulfures, (4) sauf dans les cas où des indices d'une source locale de S existent, des sulfures ou des enrichissements en éléments chalcophiles ne sont rarement ou jamais présents dans les composantes volcaniques, même là où il y a minéralisation dans le réseau de plomberie subvolcanique et (5) certaines laves sont légèrement à fortement appauvries en EGP >>> Cu > Ni > Co, ce qui indique que des sulfures qui ne se sont pas rendus à la surface ont capturé des EGP en profondeur. Deux solutions potentielles à ce paradoxe sont (*i*) que les systèmes naturels contenaient des surfactants qui réduisaient les tensions interfaciales, permettant aux bains sulfurés de coalescer et se déposer plus facilement que ce que les études théoriques et expérimentales de systèmes artificiels ou analogues prédiraient ou (*ii* que des sulfures existaient non pas sous forme de gouttelettes uniformément dispersées, comme cela est normalement présumé, mais sous forme de pseudobouchons ou pseudocouches cohérents sur le plan dynamique, qui étaient assez grands et denses pour ne pas être transportés vers le haut. Quelle que soit l'explication correcte, il semble probable que la plupart des gisements riches en sulfures à Ni–Cu–EGP dans les GPI se soient formés au niveau stratigraphique où ils se trouvent ou au-dessus. [Traduit par la Rédaction]

Mots-clés : gisements de Ni–Cu–PGE, sulfures magmatiques, complexes de grandes provinces, ignées.

Introduction

Geological, geochemical, isotopic, thermodynamic, and fluid dynamic constraints require that the sulfide in most high-grade magmatic Ni–Cu–PGE deposits in large igneous provinces (LIPs) (e.g., Circum-Superior, Eastern Goldfields, Kola, Mid-Continent Rift, Siberia, and Superior) formed by incorporation of S from crustal rocks during lava/magma emplacement (Arndt et al. 2005; Barnes and Lightfoot 2005; Keays and Lightfoot 2010; Lesher 1989,

Received 2 July 2018. Accepted 23 February 2019.

Paper handled by Guest Editor Marie-Claude Williamson.

C.M. Lesher. Mineral Exploration Research Centre, Harquail School of Earth Sciences, Goodman School of Mines, Laurentian University, Sudbury, ON P3E 2C6, Canada.

Email for correspondence: mlesher@laurentian.ca.

[1]This paper is part of a Special issue entititled "Magmatic and metallogenic processes associated with large igneous provinces".

2017; Lesher and Groves 1986; Naldrett 2004; Ripley and Li 2013). Because the solubility of sulfide in silicate melts is so low (typically <2000, often <1000 ppm: see e.g., Smythe et al. 2017), only very small amounts of sulfide could have dissolved and any excess must have initially existed as Ni–Cu–Co–PGE-poor Fe-rich sulfide xenomelts that were upgraded through interaction with the magma during transport and emplacement (Lesher and Burnham 2001; Lesher and Campbell 1993).

Despite the broad consensus on the need to incorporate crustal S to generate high-grade Ni–Cu–PGE deposits in LIPs, there are significant uncertainties regarding from where, in which direction, and how far sulfides can be transported. The preferential localization of Fe–Ni–Cu–PGE sulfides within the horizontal components of dike–sill–lava flow complexes in LIPs indicates that they were fluid dynamic traps for sulfide melts (Lesher 2017). Many models involve formation at depth with vertical transport to higher levels (e.g., Arndt et al. 2003; Barnes et al. 2016; Barnes and Robertson 2019; De Waal et al. 2004; Lesher et al. 1981; Lightfoot and Evans-Lamswood 2015; Lightfoot et al. 2012; Naldrett 2011), but there are several problems with such models.

(1) Fe–Ni–Cu sulfide melts (4.0–5.2 g/cm^3) are much denser than most silicate magmas (2.6–2.8 g/cm^3) and most crustal rocks (2.7–2.9 g/cm^3), which limits the amount of sulfide that can be transported in buoyantly rising magmas to 10%–15% (e.g., Lesher 2017; Lesher and Groves 1986) or less if any olivine is being transported (see Barnes et al. 2016).
(2) Felsic xenoliths may reduce the bulk density of the magma (and if abundant enough may also increase bulk viscosity) enough to allow the magma to transport greater amounts of sulfides (Lesher 2017), but komatiite-associated Ni—Cu–PGE deposits contain few xenoliths; the xenoliths that are present in basaltic systems are often as dense or denser than the magma (originally or after thermal metamorphism: see Mariga et al. 2006; Samalens et al. 2017), and where well characterized (e.g., Duluth, Norilsk, Voisey's Bay), they appear to be nearby country rocks, not deeper crustal rocks.
(3) S isotope data suggest that the S in most LIP-related deposits was derived from nearby rather than deeper crustal sources (e.g., Lesher 2017; Lesher and Groves 1986; Ripley and Li 2013). This does preclude contributions of S from deeper sources, but there are very few if any cases where a significantly deeper source is required. Even at Nebo-Babel and Jinchuan, which have near (but not quite exactly) mantle S isotopic ratios and where it has been emphasized in the past that no local S sources are present (Ripley et al. 2005; Seat et al. 2007), S-bearing lithologies have since been found within the same sequence at Nebo-Babel (Karykowski et al. 2015) and in the open pit at Jinchuan (E.M. Ripley, personal communication, 2012). In any case, near-zero ‰ $\delta^{34}S$ or ‰ $\Delta^{33}S$ values do not preclude an unfractionated crustal source or exchange with the magma at intermediate to high magma to sulfide ratios (Lesher et al. 1999; Lesher and Stone 1996).
(4) In many deposits, there is no mineralization outside the ore zones. If magmas were emplaced carrying sulfides, regardless of whether mantle-derived, exsolved during ascent or produced by incorporation of crustal sulfur, then all facies of the host units should have been saturated in sulfide and should contain at least some disseminated mineralization: (*i*) sulfides should have been trapped in the chilled margins of the host units, (*ii*) sulfides should have continued to exsolve throughout host units as the lavas/magmas cooled, oxidized, and crystallized after emplacement, and (*iii*) crystallization of sulfide-saturated lavas/magmas should have resulted in significant accumulation of sulfide with cumulus silicates (Lesher and Groves 1986).
(5) Despite being characterized by very high eruptive rates up to 2000–4000 m^3/s[1] (e.g., Self et al. 2014), the eruptive components of LIPs contain essentially no sulfides except where there is geological, stratigraphic, geochemical, and isotopic evidence that the sulfides formed at that stratigraphic level (e.g., Abitibi, Eastern Goldfields, Raglan, and Zimbabwe), even when the subvolcanic plumbing system contains mineralization (e.g., Emeishan, Mid-Continent Rift, Pechenga, Siberia, and Thompson Nickel Belt).
(6) On the other hand, parts of some LIPs (up to 5000 km^3 or more) are moderately to strongly depleted in PGE >> Cu > Ni > Co (e.g., Arndt et al. 2003; Brügmann et al. 1993; Keays and Lightfoot 2015; Lightfoot et al. 1997; Song et al. 2009*a*), indicating that sulfides sequestered PGEs at depth and that those sulfides were not erupted.

Together, these points suggest that Fe–Ni–Cu–PGE sulfide melts are rarely if ever transported upwards. The aim of this paper is to discuss the transport of sulfides in the plumbing systems of mineralized LIPs and to place constraints on the sources of the sulfides and the direction that they were transported.

Magmatic Ni–Cu–PGE deposits in LIPs

Magmatic Ni–Cu–Co–PGE deposits can be subdivided into (1) high-sulfide Ni–Cu–Co–(PGE) deposits mined primarily for their Ni–Cu–Co contents (e.g., Pechenga, Voisey's Bay and many Chinese deposits), (2) high-sulfide Ni–Cu–Co–PGE deposits mined for their Ni–Cu–Co contents but with PGE as significant by-products (e.g., Bushveld Platreef and Flatreef, Duluth, Jinchuan, Kambalda, Norilsk, Perseverance, Raglan, Sudbury, and Thompson), and (3) low-sulfide PGE–(Cu)–(Ni)–(Co) deposits mined primarily for their PGE contents (e.g., PGE reefs in Bushveld, Jinbaoshan, and Stillwater) (Lu et al. 2019). This paper is concerned only with the first and second groups, referred to here for simplicity as Ni–Cu–PGE deposits.

Many of the world's largest Ni–Cu–PGE deposits are hosted by LIPs, which have been defined as magmatic provinces with intraplate tectonic settings or geochemical affinities, large areal extents (>100 000 km^2) and volumes (>100 000 km^3), and short lifespans (~50 Myr), where a large proportion (>75%) of the total igneous volume was emplaced over a very short time interval (1–5 Myr) (Bryan and Ernst 2008; Ernst 2014). LIPs are interpreted to be products of large-scale melting during the arrival of the heads of starting plumes, as opposed to ongoing melting from the plume tail, which produces seamount chains and other hot spot tracks (e.g., Campbell and Griffiths 1990). Thus, seamounts, seamount groups, submarine ridges, and anomalous seafloor crust are not considered to be LIPs, but giant mafic continental dyke or sill intrusive provinces and Archean greenstone tholeiite–komatiite associations are included (Bryan and Ernst 2008).

Not all LIPs are mineralized (e.g., Ernst and Jowitt 2013; Jowitt and Ernst 2013; Zhang et al. 2008) and not all LIPs are equally mineralized, but LIPs are a favoured host for magmatic Ni–Cu–PGE mineralization because they provide (by definition) anomalously high magma fluxes (e.g., Self et al. 2014; White et al. 2006) and because high magma fluxes facilitate thermomechanical erosion of wall rocks and incorporation of crustal S (e.g., Arndt et al. 2005; Barnes and Lightfoot 2005; Barnes et al. 2016; Lesher 1989; Williams et al. 1998).

Table 1 lists and Fig. 1 shows LIPs where intrusives and (or) lavas contain known mineralization. Several points are evident.

(1) Mineralized LIPs occur throughout geological time in a variety of tectonic settings in association with a wide range of magma compositions. The proportion of LIPs that are mineralized appears to be highest in the Archean, intermediate in the Protoerozoic, and least in the Phanerozoic, but deposit sizes also increase with time. In any case, age, tectonic setting, and magma composition do not appear to be important controls on the formation of magmatic Ni–Cu–PGE deposits.
(2) Archean deposits are associated primarily with komatiitic magmas, Proterozoic deposits are associated primarily with

Table 1. Ages, inferred tectonic settings, magma types, mineralization status of comagmatic intrusions and lavas, and sources of xenoliths, contamination, and S for selected Ni–Cu–PGE deposits in large igneous provinces (LIPs).

LIP	Tectonic setting	Magma type	Mineralized intrusions	Mineralized lavas	Xenoliths	Contamination	S source(s)	Selected reference(s)
Pilbara 3270–3250 Ma	Greenstone belt	Basaltic	Mt Scholl Radio Hill	None known	None reported			De Angelis et al. 1987
	Greenstone belt	Al-depleted komatiite	None known	Ruth Well (unrelated)	None reported			Nisbet and Chinner 1981
Forrestania – Lake Johnson 2900 Ma	Greenstone belt	Al-depleted komatiite	Cosmic Boy Digger Rocks New Morning Flying Fox Emily Ann Maggie Hays	None known	Local OXIF and Qtz-Mica schist		Local SUIF*?	Porter and McKay 1981; Perring et al. 1995, 1996; Frost et al. 1998; Barnes 2006
Abitibi-Wawa 2750–2724 Ma	Greenstone belt	Al-undepleted komatiite	Shebandowan Dundonald McWatters Sothman Dumont Grasset?	Alexo Hart-Langmuir-Redstone-Texmont-Bannockburn Marbridge	Rare local	Local rocks ± upper crust	Local SUIF and argillite	Sproule et al. 2002; Houlé and Lesher 2011 ; Houlé et al. 2018
Bird River – Uchi – Oxford-Stull – La Grande – Eastmain 2730 Ma	Greenstone belt	Al-undepleted komatiite	Eagle's Nest Blue Jay	None known, but poorly exposed	Underlying SUIF*	Local rocks ± upper crust	Local SUIF and an undiscovered source	Mungall et al. 2010; Houlé et al. 2013
Bulawayan-Belingwe 2700 Ma	Greenstone belt	Al-undepleted komatiite	None known	Damba-Silwane Epoch Hunter's Road Shangani Trojan	Underlying OXIF			Prendergast 2003
Eastern Goldfields 2700 Ma	Greenstone belt	Al-depleted komatiite	Honeymoon Well Yakabindie	Kambalda Camp Widgiemooltha Camp Mt Keith Perseverance	Rare local	Local rocks ± upper crust	Local sulfidic cherts, argillites, felsic volcanics	Lesher 1989; Barnes 2006
Matachewan 2480–2450 Ma	Rifted continental margin	High-Al basalt	East Bull Lake River Valley	None known	Local	Local		Peck et al. 2001; James et al. 2002; Holwell et al. 2014
Nipissing 2217–2210 Ma	Rifted continental margin	Tholeiitic basalt	Shakespeare	None known	Quartzite and rare diorite	Local and proximal		Lightfoot and Naldrett 1996; Sproule et al. 2005
Bushveld 2060 Ma	Layered intrusion	Contaminated komatiite or siliceous high-magnesian basalt	Bushveld	None known	Local on North Limb (Platreef and Flatreef)	Local on North Limb (Platreef and Flatreef)	Magma (Merensky Reef) and crustal (Platreef and Flatreef)	Kinnaird et al. 2005; Wilson 2012; Maier et al. 2013
Pechenga–Onega 1970 Ma	Rifted continental margin	Ferropicrite	Other Pechenga	Kotselvaara Kammikivi Semiletka	Rare semipelite	Local rocks ± upper crust	Underlying semipelite	Barnes et al. 2001
Circum-Superior 1880 Ma	Rifted continental margin	Komatiitic basalt and Al-undepleted komatiite	Expo-Méquillon Thompson Camp Labrador Trough	Raglan Camp	Rare local	Local rocks ± upper crust	Adjacent semipelites and SUIF	Layton-Matthews et al. 2007; Lesher 2007; Mungall 2007
Nain 1300 Ma	Rifted continental margin	High-Al–Fe basalt?	Voisey's Bay	Not exposed	Local	Local paragneisses and orthogneisses	Local gneisses	Lightfoot et al. 2012; Scoates and Mitchell 2000
McKenzie 1267 Ma	Continental rift	Tholeiitic basalt	Muskox	None known				Hulbert 2005; Irvine and Smith 1967
Keweenawan 1115–1085 Ma	Continental rift	Tholeiitic basalt	Duluth Eagle Tamarack Current Lake	None known	Local and cognate	Adjacent pelites and OXIF	Local pelite	Miller 2011; Ding et al. 2012*a*; Taranovic et al. 2015
Warakurna 1078–1070 Ma	Continental rift	Tholeiitic basalt	Giles Complex Nebo-Babel	None known	Adjacent felsic orthogneiss	Adjacent felsic orthogneiss	Reported to be mantle but likely recently recognized sulfidic sediments	Maier et al. 2015; Seat et al. 2007; Wingate et al. 2004
Gubei 825 Ma	Rifted continental margin	Picrite or ferropicrite	Jinchuan	Not exposed	Rare local	Local marble and paragneiss ± upper crust	Not clear	Li and Ripley 2011
Dovyren-Kingash 725 Ma			Dovyren Kingash	None known				Ariskin et al. 2016; Polyakov et al. 2013
Franklin 710–730 Ma		Tholetiitic basalt	Southern Feeder Dike Complex	None known	Diabase (cognate)	Adjacent rocks	Adjacent rocks	Hayes et al. 2015
Emeishan 262–261 Ma	Continental rift	Low-Ti picrite	Baimazhai Limahe Yangliuping Zubu	None known	Rare local	Local rocks ± upper crust	Not clear	Zhou et al. 2002; Wang et al. 2018
Wrangelia 231–225 Ma	Oceanic plateau	Picrite–tholeiitic basalt	Wellgreen	None known				Hulbert 1997; Schmidt and Rogers 2007
Tarim 209 Ma	Back arc	Basalt	Kalatongke Maksut	None known				Li et al. 2012
Siberia 205 Ma	Continental rift	Picrite	Norilsk-Talnakh	None known	Adjacent evaporite and argillite	Local rocks ± lower crust	Local evaporite and argillite	Arndt et al. 2003; Naldrett et al. 1995
Central Atlantic 200 Ma	Continental rift	High-Ti tholeiitic basalt	Freetown	None known				Callegaro et al. 2017; Chalokwu et al. 1995
Karoo 183 Ma	Continental rift	Basalt	Insizwa	None known				Lightfoot and Naldrett 1983, 1984

*SUIF, sulfide–facies iron formation.

Fig. 1. Variations in MgO content of mantle-derived magmas with time (expanded from Campbell and Griffiths 1992, 2014). [Colour online.]

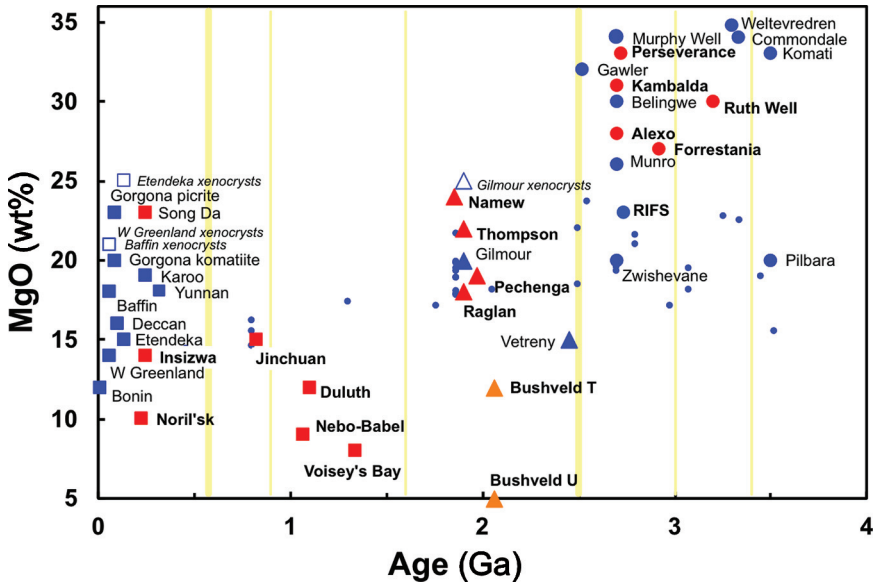

komatiitic basaltic or ferropicritic magmas, and Phanerozoic deposits are associated primarily with picritic and basaltic magmas.

(3) Archean deposits are most commonly extrusive, Proterozoic deposits are sometimes intrusive and sometimes extrusive, and Phanerozoic deposits are exclusively intrusive.

(4) All of the listed areas contain mineralized intrusions, but not all areas contain mineralized lavas. Komatiite, ferropicrite, and komatiitic basalt lavas contain Ni–Cu–PGE mineralization, but picrite and basalt lavas are uniformly barren even if occurring in similar geological or stratigraphic settings.

(5) Where lavas are mineralized, there is field, geochemical, and (or) S–Pb–Os isotopic evidence that the sulfides formed at that stratigraphic level (see reviews by Barnes 2006; Lesher 1989; Lesher 2007; Lesher and Keays 2002).

(6) Where xenoliths are present, they appear to be derived from nearby or adjacent country rocks, not deeper crustal rocks.

(7) Almost all deposits appear to have incorporated S from nearby or adjacent country rocks (see Lesher 2017; Lesher and Groves 1986; Ripley and Li 2013).

Host units

Geometries

Lesher (1989), Barnes (2006), and Arndt et al. (2008) have summarized the geometries of mineralized extrusive and intrusive units hosted by komatiitic rocks, and Mao et al. (2008), Lightfoot and Evans-Lamswood (2015), Barnes et al. (2016), Barnes and Mungall (2018), and Lu et al. (2019) have summarized the geometries of mineralized intrusive units hosted by basaltic rocks. Examples are listed in Table 2 in terms of inferred original geometry and orientation.

Subhorizontal extrusive and intrusive bodies can be geometrically similar, so they have been combined for simplicity. Some of the subdivisions of Lightfoot and Evans-Lamswood (2015) and Barnes and Mungall (2018) have been combined, as they likely represent different erosional levels of similar structures (see, e.g., Mao et al. 2008). For example, subhorizontal linear funnels and elongate boat-shaped features may be erosional remnants of subhorizontal blade-shaped dikes and subhorizontal troughs may be erosional remnants of subhorizontal chonoliths.

Most of the assignments are similar to those in Lightfoot and Evans-Lamswood (2015), Barnes et al. (2016), and Barnes and Mungall (2018) with two significant exceptions.

(1) Tang (1993) and Lightfoot and Evans-Lamswood (2015) interpreted the Jinchuan intrusion as a subvertical funnel, whereas Lehmann et al. (2007), Song et al. (2009*b*), and Song et al. (2012) interpreted it as a structurally rotated sill. The observations of Lehmann et al. (2007) regarding rotation of an overlying disconformity are compelling and such a model is consistent with (*i*) the weak asymmetric differentiation (wehrlite/feldspathic lherzolite/lherzolite/harzburgite/wehrlite) in the main segment of the intrusion (Tonnelier 2010), (*ii*) the broadly symmetric distribution of mainly net- and patchy-net-textured mineralization in the main central part of the system but broadly asymmetrically distributed massive\net\disseminated mineralization in the lateral (northwestern and southeastern) parts of the intrusion (Tonnelier 2010), and (*iii*) the presence of abundant hydrothermal quartz veins oriented normal to the upper (southwestern) contact, and their absence along the lower (northeastern) contact (C.M. Lesher, unpublished data). The weight of evidence is therefore toward it being a subhorizontal sill, but if not rotated, then it is more likely a subhorizontal blade-shaped dike than a funnel (see below).

(2) Branquet et al. (2012) interpreted the host units in the East Tianshan district of China as syn-kinematic sheeted intrusions and Lightfoot and Evans-Lamswood (2015) interpreted them as trans-tensional subvertical funnels. Barnes and Mungall (2018) noted that many of these could also be blade-shaped dikes and Lu et al. (2019) have suggested the same based on their asymmetric differentiation, so they have been classified here as originally subhorizontal blade-shaped dikes.

Regardless of the finer details, several features are evident in Table 2.

(1) The mineralized units exhibit a wide range of length (L), width (W), and height (H) ratios. Barnes and Mungall (2018) suggested that there is a continuum between blade-shaped dikes ($L >> H > W$) and tube-like chonoliths ($L >> W \sim H$), but there is also clearly a continuum between chonoliths, channelized flows/sills ($L >> W > H$), and channelized sheet flows/sills ($L >> W >> H$), as shown in Fig. 2.

(2) Subhorizontal units are much better mineralized than subvertical units.

(3) Deposits in channelized flows/sills and channelized sheet flows/sills tend to be larger and higher grade than deposits in

Table 2. Subdivision of selected extrusive and intrusive mineralized units in terms of original orientation, morphology, and degree of differentiation (expanded and modified from Mao et al. 2008; Lightfoot and Evans-Lamswood 2015; Barnes et al. 2016; Barnes and Mungall 2018, and references therein).

	Asymmetrically differentiated		
Orientation/morphology	Weakly differentiated	Moderately to strongly differentiated	Symmetrically differentiated
Subhorizontal blade ± funnel	Eagle's Nest* Expo-Ungava Méquillon	Hongqiling Huanshanan Huanshandong Huanshanxi Kalatongke Limahe Tabankulu (Mt. Ayliff) Ovoid (Voisey's Bay) Discovery Hill (Voisey's Bay) Qingquanshan Xiangshan	None known
Subhorizontal channel/trough/chonolith	Jinchuan* Raglan Mt Keith Thompson	Duluth Limoeiro Nebo-Babel Pechenga Lower Talnakh NE Talnakh Tamarack Uitkomst Xiarihamu	None known
Subhorizontal channelized sheet	Kambalda Perseverance	Insizwa (Mt Ayliff) Kharaelakh (Norilsk) Norilsk I Talnakh	None known
Subhorizontal sheet	None known	None known	None known
Subvertical pipe	None known	None known	Giant Mascot Jingbulake Tulameen?
Subvertical blade	Reid Brook (Voisey's Bay)	None known	None known
Subvertical sheet	None known	None known	None known

*After allowance for structural rotation.

Fig. 2. Morphological continuum between (A) undifferentiated, (B) noncumulate differentiated, (C) cumulate differentiated, and (D) cumulate undifferentiated blade-shape dikes (*i*), various shapes of chonoliths (*ii–vi*), and blade-shaped sills (*vii*). Chilled margins, sheet dikes, and sheet sills are not shown. Only cumulate differentiated (Fig. 2C) and cumulate undifferentiated (Fig. 2D) bodies host significant amounts of mineralization. [Colour online.]

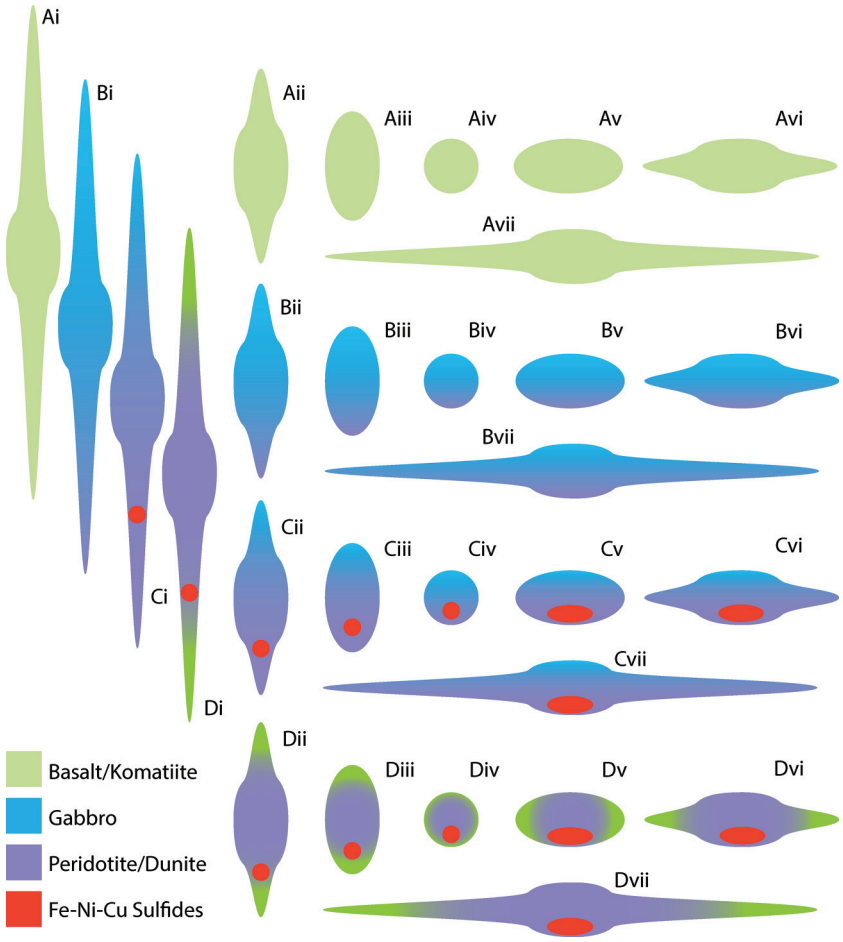

blade-shaped dikes and tube-like chonoliths, but all host economically significant Ni–Cu–PGE deposits.

(4) Few Ni–Cu–PGE deposits occur in unchannelized dikes ($L \sim H >> W$) or unchannelized sills ($L \sim W >> H$). The offset dikes at Sudbury are a major exception, but Sudbury is not a LIP and they were emplaced extremely rapidly after a major impact event (see review by Lightfoot 2016). There is mineralization in the sloping Reid Brook dike at Voisey's Bay but less than in the subhorizontal parts of the system and that present is often in subhorizontal structures (Evans-Lamswood et al. 2000).

Fig. 3. Variation in relative degrees of Ol ± Pyx enrichment and differentiation of mafic–ultramafic flows, sills, chonoliths, and dikes (modified from Lesher et al. (1984); Lesher and Keays (2002)). UN, undifferentiated noncumulate (massive, pillowed, or volcaniclastic); DN, differentiated noncumulate; DC, differentiated cumulate; UC, undifferentiated cumulate. [Colour online.]

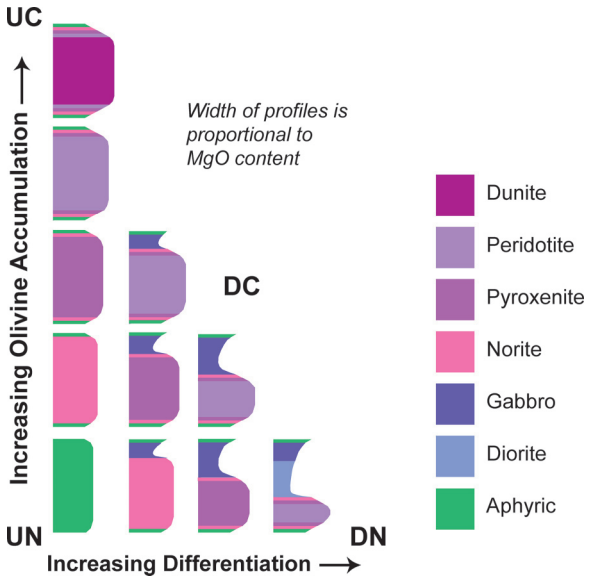

Cumulate versus noncumulate units

All mineralized units contain some degree of excess cumulus Ol ± Pyx, in some cases very significant amounts (Figs. 2 and 3). Some authors have interpreted this to indicate that the magmas transported significant amounts of intratelluric phenocrysts (e.g., De Waal et al. 2004), but many exhibit textures (e.g., crescumulate) and (or) systematic compositional variations more compatible with crystallization in situ (e.g., Barnes et al. 2019; Lesher 1989, 2007; Mao et al. 2018). This and other geological, mineralogical, geochemical, and (or) isotopic evidence suggest that most were open systems involving semicontinuous or multiple discrete phases of magma emplacement and in situ crystallization.

Degree of differentiation

Some host units are weakly differentiated and composed mainly of dunite ± peridotite ± pyroxenite (e.g., Jinchuan, most Kambalda host units, Mt Keith, Perseverance, Raglan, and Thompson), whereas others are more strongly differentiated and composed of dunite ± peridotite ± pyroxenite ± gabbro ± diorite (e.g., Duluth, Norilsk, Pechenga, Tamarack, and most Chinese deposits other than Jinchuan and Xiarihamu) (Table 2; Figs. 2 and 3). Poorly differentiated, olivine-rich bodies are hallmarks of lava/magma channelization and flow-through olivine ± pyroxene accumulation after sulfide generation/deposition (e.g., Arndt et al. 2008; Barnes 2006; Lesher 1989; Lesher et al. 1984), but it is possible for a channelized system to pond (cease flow-through) and differentiate shortly after sulfide generation/deposition (see discussion in Arndt et al. 2008; Lesher 1989). Some of the latter bodies may be distinguished as highly channelized systems by their geometries and wider-than-normal contact metasomatic aureoles (e.g., Norilsk-Talnakh: Lightfoot and Zotov (2014; Zotov 1976), keeping in mind that the rate of heat conduction into wall rocks is orders of magnitude slower than the rates of magma flow-through and thermomechanical erosion (e.g., Barnes and Robertson 2019; Huppert and Sparks 1985; Williams et al. 1998).

In most cases, the differentiation is asymmetric (Table 2; Figs. 2 and 3), consistent with magmatic crystallization in a gravitational field and therefore with a current or original subhorizontal orientation. Only a few deposits (e.g., Jingbulake, many Uralian–Alaskan-type intrusions) are concentrically differentiated, consistent with them being emplaced as subvertical funnels/pipes ($H >> L \sim W$). These contain low-sulfide PGE–(Cu)–(Ni) mineralization (e.g., Nixon et al. 2015) but rarely contain significant amounts of Ni–Cu–PGE mineralization.

Magma transport and emplacement

Most magmas rise through the crust because of buoyancy (e.g., Lister and Kerr 1991; Wilson and Head 1981). Some may be driven upwards by seismic pumping (e.g., Maier et al. 2016) or roof foundering (e.g., Saumur et al. 2015), but the magmas in LIPs are much too voluminous to have been influenced by such processes and almost certainly rose because of buoyancy.

The buoyant ascent rate will increase with increasing density of the crust, decreasing density of the magma, increasing width of the conduit or fissure, and decreasing viscosity of the magma. None of these parameters are known and some will change with time and location in the system, but we can assume that ascent velocities of the magmas that generated LIPs were of the order of 1–10 m/s (e.g., Huppert and Sparks 1985; Wilson and Head 1981), higher and more voluminous in areas where density and rheological contrasts were greater, and lower and less voluminous in areas where density and rheological contrasts were smaller (e.g., Abitibi versus Thompson versus Norseman–Wiluna: Houlé et al. 2008); Layton-Matthews et al. 2010); Lesher and Keays 2002)) and (or) where tectonic conditions were more favourable (Barnes and Fiorentini 2012).

The morphology of the conduit (Fig. 2) will depend on stresses and rheological controls (e.g., Lister and Kerr 1991; Menand 2011; Townsend et al. 2017). As noted above, the precise geometry is not particularly important; what is important is the degree of channelization.

The relative timing of emplacement of intrusions and lavas is not well constrained in many areas, but some intrusions predate volcanism (Mungall 2007), some were emplaced during volcanism (Burgess and Bowring 2015), and some postdate volcanism (Paces and Miller 1993).

Sulfide transport

Fe–Ni–Cu sulfide melts are very dense (4.0–5.2 g/cm^3: Dobrovinski et al. 1969; Mungall and Su 2005) and very fluid (0.01–0.1 Pa s: Dobson et al. 2000) compared to mafic–ultramafic silicate melts (2.7–2.9 g/cm^3 and 1–100 Pa s: e.g., Williams et al. 1998).

Vertical transport

Sulfides can be transported upwards in magmas in several different ways.

(1) *In solution*: This is limited by the low solubility of S in mafic–ultramafic magmas (e.g., Smythe et al. 2017) and the small amounts of sulfide that can exsolve during crystallization, contamination, or magma mixing (see Li and Ripley 2005).

(2) *Dispersed mist*: In theory, transporting very fine sulfide droplets is limited to some degree by the negative P dependence on S solubility (Mavrogenes and O'Neill 1999; Wendlandt 1982). For example, S solubility increases by ~650 ppm (~0.17% sulfide) over a pressure drop of 50 kbar (167 km), by ~390 ppm (~0.10% sulfide) over a pressure drop of 30 kbar (100 km), by ~260 ppm (~0.07% sulfide) over a pressure drop of 20 kbar (67 km), and by ~130 ppm (~0.03% sulfide) over a pressure drop of 10 kbar (17 km). However, Robertson et al. (2015*b*) noted that dissolution rates are very slow compared to transport rates, especially for fine droplets, and concluded that the extent of dissolution during vertical transport, even over large (~10 km) distances, is likely to be negligible.

(3) *Dispersed droplets*: Theoretical and analog experimental studies have shown that small (<1–2 cm) droplets can be transported at typical magma ascent velocities as dilute (<10%–15%) suspensions (De Bremond d'Ars et al. 2001; Lesher 2017;

Fig. 4. Maximum settling velocities (estimated using Stokes' Law) versus diameter for chromite, olivine, sulfide melt, mafic xenoliths with and without 10% sulfide melt, and felsic xenoliths with and without 10% sulfide melt compared to typical magma ascent velocities (0.1–10 m/s). Boxes show settling rates for common grain/droplet/xenolith sizes. Magma density assumed to be 2.7 g/cm^3 and magma viscosity assumed to be 100 g·cm^{-1}·s^{-1}. Modified from Lesher (2017). [Colour online.]

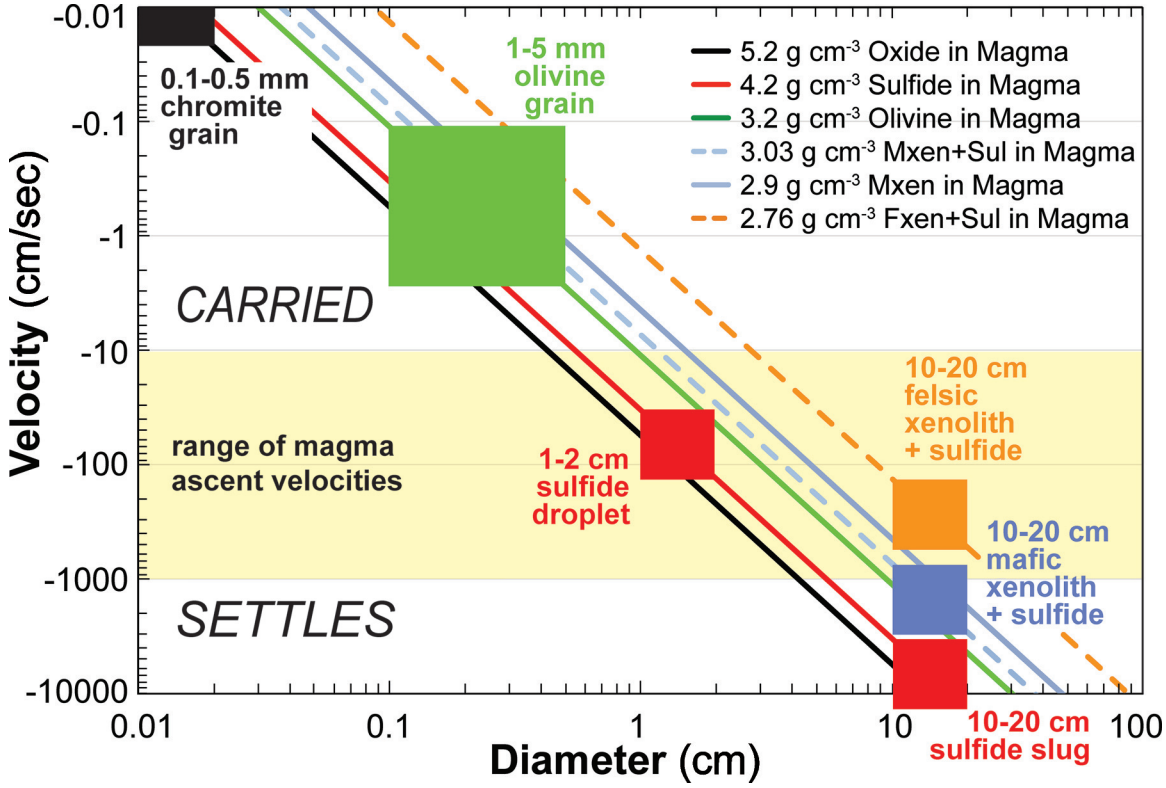

Lesher and Groves 1986; Robertson et al. 2015*b*) (Fig. 4) but will settle at lower velocities (e.g., Hughes et al. 2016).

(4) *Droplets carried by crystals or xenoliths*: Xenoliths will increase the amount of sulfide that can be transported if the xenoliths are less dense than the magma (Lesher 2017). However, a 5–10 cm felsic xenolith of density 2.6 g/cm^3 carrying 10% sulfide of density 4.2 g/cm^3 will settle at the same rate as a 1–2 cm sulfide droplet (Fig. 4), so this would only be an efficient way to transport sulfide if the xenoliths are smaller and (or) less dense than assumed in these calculations. The density of olivine is always greater than the magma (Fig. 4) so would not be a very effective transporting mechanism.

(5) *Droplets carried by gas bubbles*: Gas bubbles reduce bulk density significantly (Barnes et al. 2019; Lesher 2017; Mungall et al. 2015) and would greatly enhance transport. Although there are a few places where sulfide droplets appear to have been floated by vesicles (e.g., Eckstrand and Williamson 1985; Stone et al. 1996), in places where they are more abundant (e.g., Black Swan, Kambalda, and Norilsk), they occur mainly within the central parts of the mineralized units. Importantly, as noted above, at Norilsk, there are no metal enrichments in any of the erupted lavas.

(6) *Slug flow*: This is limited by the very high density of sulfide. Slugs greater than ~10 cm cannot be transported in magmas ascending at even the highest estimated flow rates (Lesher 2017) (Fig. 4).

(7) *Tectonic pumping*: This is probably only way to transport massive sulfide melts upwards. Normal plate tectonic processes are too slow. Earthquake-driven seismic pumping (e.g., Maier et al. 2016) and graben collapse (e.g., Cruden et al. 2000) are rapid enough, but as noted above, the magmatism in LIPs is most likely driven by buoyancy, not tectonic processes, and it is very difficult to reentrain and draw up previously segregated sulfide melts (Saumur et al. 2015). Even if one argued that this could have occurred, it is not consistent with the vast majority of deposits where there is evidence for incorporation of sulfides from local country rocks or rocks along strike.

Coalescence will increase droplet size, increase settling rates, and potentially lead to "flooding" where sulfide melt becomes the continuous phase (Fig. 5), making upward transport impossible. De Bremond d'Ars et al. (2001) argued, on the basis of scaled experiments involving denser, less viscous silicone oil droplets (sulfide melt analog) in a less dense, more viscous aqueous polymer solution (silicate melt analog), that sulfide droplets should not coalesce because they would be separated by a film of silicate melt. Robertson et al. (2015*b*) explained that this is because film drainage occurs at much longer timescales than viscous flow of the carrier magma, especially for the low Bond numbers (dimensionless ratio of gravitational and surface tension forces) that apply to the typical size range of sulfide droplets, so breakup should be more rapid than coalescence. However, the de Bremond d'Ars et al. experiments were conducted in a vertical cylinder rather than an inclined cylinder, which would facilitate segregation and flooding (Fig. 5); neither study simulated the dominantly horizontal flow in most mineralized magmatic plumbing systems, and neither prediction is consistent with the absence of sulfide droplets in overlying lavas or lateral facies of the intrusions.

The sulfides in some deposits (e.g., Platreef: Ihlenfeld and Keays 2011; River Valley: Holwell et al. 2014) have been suggested to have been derived "from depth", but few studies provide constraints on whether the source was significantly deeper or at more-or-less the same stratigraphic level.

Fig. 5. Flow patterns in vertical, subvertical, and inclined countercurrent flow Lesher (2017) as modified from Ullmann et al. (2003). [Colour online.]

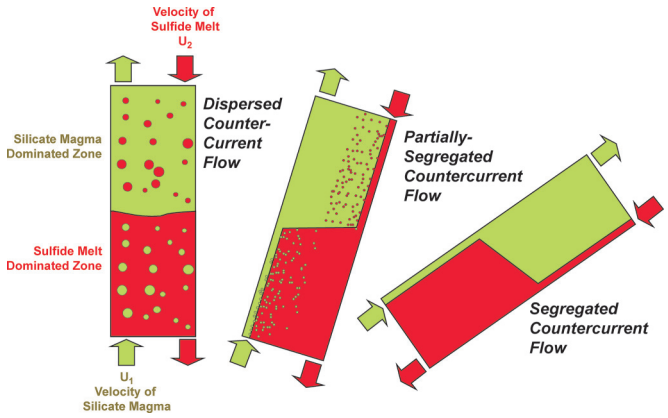

The Eagle deposit is hosted by Proterozoic intrusive rocks but the semimassive sulfides exhibit a relatively wide range (+0.8‰ to –0.8‰) of $\Delta^{33}S$ values, which have been used to infer a deeper Archean source (Ding et al. 2012*b*). However, transport of sulfides from depth does not explain how very dense, very fluid massive sulfide melts could be trapped in the throat of the host intrusion and not settle back into the conduit. Given that the Eagle intrusion occurs so close to the Archean/Proterozoic unconformity, a more likely model is that the host intrusion is a subhorizontal blade-shaped dike, like those now recognized to occur in other areas (see Barnes and Mungall 2018), that sampled the Archean rocks or perhaps even Proterozoic rocks containing a component of Archean S (V. Taranovic, personal communication, 2017; see, e.g., Young et al. 2013).

Countercurrent flow

The flow of less dense, more viscous oil (analogous to silicate melt in terms of relative density and viscosity) and denser, less viscous water (analogous to sulfide melt in terms of relative density and viscosity) has been studied extensively in the petroleum industry and fluid mechanics literature, where it has been shown that, with all else equal, the inclination of the conduit is more important than flow rate in controlling transitions between dispersed, slug, and layered countercurrent flow (e.g., Ullmann et al. 2003) (Fig. 6). Importantly, these studies have shown that the phases do not need to be segregated but may form pseudoslugs or pseudolayers that may also flow concurrently with highly variable volume fractions (e.g., Zhu et al. 2014, 2011; Zong et al. 2010) (Fig. 7B). The point is that even if sulfide droplets are broken up during turbulent flow (Robertson et al. 2015*b*), if they are abundant enough within a particular domain, the domain may still be denser than the remainder of the silicate magma. If 1 cm is the upper diameter for upward transport (De Bremond d'Ars et al. 2001; Lesher and Groves 1986; Robertson et al. 2015*b*), pseudoslugs containing 1%, 5%, and 10% sulfide would only need to be >10, >4.5, and >3.3 cm in effective diameter, respectively, to sink.

Subhorizontal transport

Because of their very high densities and very low viscosities, segregated sulfide liquids will flow laterally over even very shallow slopes under the influence of gravity, with flow rate controlled by the density and viscosity of the sulfide melt and the slope. If entrained by the silicate melt to any degree, flow rate will be controlled by the density, viscosity, and velocity of the mixture and the overlying silicate melt column, like submarine sedimentary debris flows.

An analysis of flow rates is beyond the scope of this contribution, as the above parameters will vary from system to system, within different parts of the same system, and with time. However, we can predict that at lower flow rates and laminar flow regimes, the interface between the silicate magma and sulfide melt will be more planar (Fig. 8A), at intermediate flow rates and transitional flow regimes, the interface will be more scalloped and some sulfide droplets may be entrained (Fig. 8B), and at higher flow rates and turbulent flow regimes, many sulfide droplets will be entrained (Fig. 8C) (e.g., Lesher and Campbell 1993; Robertson et al. 2015*b*). Although we now see only a snapshot at the end of the process after flow has stopped and crystallized, obscuring most of the evidence for horizontal transport, there are several observations that appear to require some degree of horizontal transport.

(1) The ores in all high-grade deposits are too abundant to have segregated by precipitation from the observed host rocks. In subhorizontal systems, this requires at least some degree of horizontal transport and concentration (e.g., Lesher and Burnham 2001).
(2) Some ores (and probably many more once more data are available) have S isotopic compositions that require contributions from stratigraphic equivalents of the local country rocks, not the immediate country rocks (e.g., Bekker et al. 2009).
(3) The ores at some deposits (e.g., Alexo and parts of Raglan) are underlain by a layer of sulfide-free host rocks. Their absence requires that the sulfides be transported from upstream in the lava channel, which is also consistent with the evidence for multistage ore emplacement at Alexo (Houlé et al. 2012) and Raglan (Lesher 2007).

Staging chambers

Many models for the formation of magmatic Ni–Cu–PGE deposits involve "staging chambers": deeper chambers in which sulfides segregated from the magma prior to its ascent to higher levels.

(1) In some cases, a staging chamber is invoked to provide a source for massive sulfides that cross-cut other mineralized rocks (e.g., Tang 1993). However, sulfides crystallize to lower temperatures (see review of phase equilibria by Naldrett 2004) than the silicates in mafic–ultramafic magmas, so it is just as likely that many of the massive sulfides represent mobilization of molten sulfides during crystallization of the intrusion (e.g., Barnes et al. 2016; Tonnelier 2010).
(2) In some cases, a staging chamber is invoked to explain lower- or higher-than-expected PGE contents in the ores (e.g., Lightfoot and Keays 2005; Song et al. 2008; Song et al. 2006). However, in most cases, such variations can also be explained by a combination of variations in source composition (Lu et al. 2019; Tonnelier 2010; Tonnelier et al. 2013), degree or mode of partial melting (batch versus dynamic versus fractional), magma to sulfide ratio (*R* factor), and (or) degree of MSS fractionation/accumulation.
(3) In some cases, a staging chamber is invoked to explain inclusions containing compositionally similar mineralization (e.g., Holwell et al. 2014; Sproule et al. 2005). However, in many cases, the inclusions may be anteliths ("cognate xenoliths") derived from upstream in the system and not necessarily from depth.

The problems associated with transporting dense sulfides from deeper staging chambers are magnified, as any sulfides that formed must be reentrained. Saumur et al. (2015) investigated this process experimentally and theoretically and concluded that highly dynamic magmatic conditions are required to achieve significant draw-up of sulfide and that draw-up heights would in any case not be very large (≤4 m), eliminating this as a process in all but the thinnest intrusions. They also noted that draw-up would be favoured in intrusions subjected to large pressure gradients

Fig. 6. Mechanisms for horizontal transport of sulfides in laminar, transitional, and turbulent flow regimes (based on Lesher and Campbell 1993)). [Colour online.]

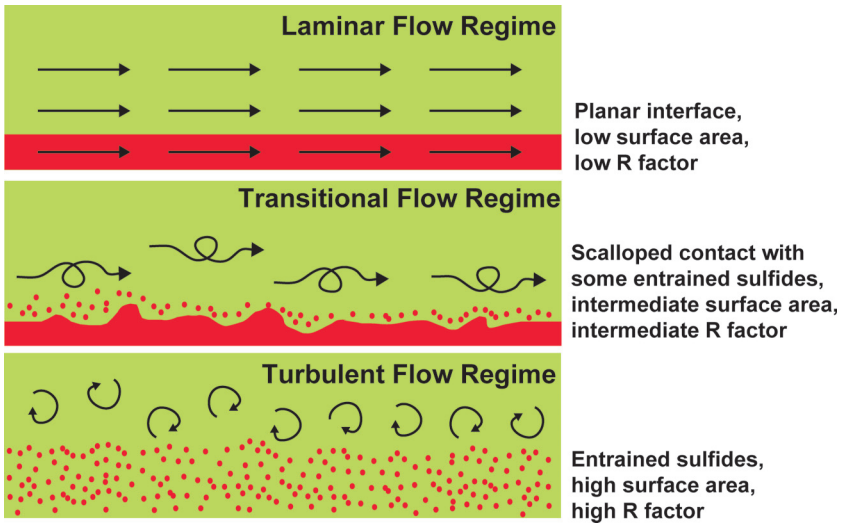

Fig. 7. PGE contents of magmas carrying 0.01%–3% sulfide droplets showing strong degrees of enrichment, even if very small amounts are present and if S is devolatilized. [Colour online.]

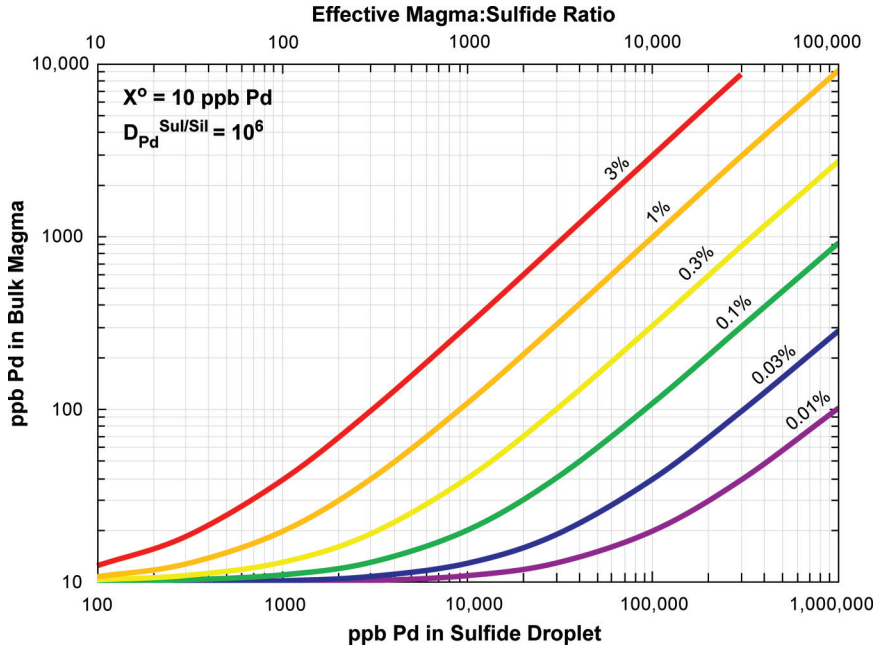

(e.g., pressures associated with foundering of the roof during cauldron subsidence or magma overpressure such as expected in mid- to upper-crustal intrusive systems) but not in subvolcanic systems that may not exhibit high enough lithostatic pressures on the plumbing system to generate high pressure gradients, drive high magma flow rates, and produce upward sulfide entrainment. Draw-up in inclined systems would presumably be easier but is still not without problems, as noted above.

Discussion

Absence of sulfides in lavas overlying mineralized intrusions

The paradox of why fine (≤1 cm) Fe–Ni–Cu–PGE sulfide droplets should be transportable at normal magma ascent rates and occur so often in subvolcanic intrusions but almost never (if ever) occur in the thick sequences of rapidly erupted volcanic rocks that overlie the intrusions may have several possible explanations.

(1) The mineralized intrusions may have intruded after the volcanic rocks. This happened in some cases (e.g., Duluth: Paces and Miller 1993) but is unlikely to have occurred in all cases, particularly at Norilsk where the mineralized intrusions have been geochemically and geochronologically linked to overlying volcanic rocks (e.g., Burgess and Bowring 2015; Czamanske et al. 1994; Czamanske et al. 1995; Fedorenko 1994; Radko 2016).

(2) The mineralized intrusions may correlate with unexposed and (or) unsampled volcanic rocks. This is always possible, and several authors have argued against links between the mineralized intrusions at Norilsk and immediately overlying lavas (e.g., Latypov 2002; Ripley et al. 2003). However, many

Fig. 8. Flow patterns in inclined pseudolayered and pseudoslug countercurrent flow (modified from Zhu et al. 2014). [Colour online.]

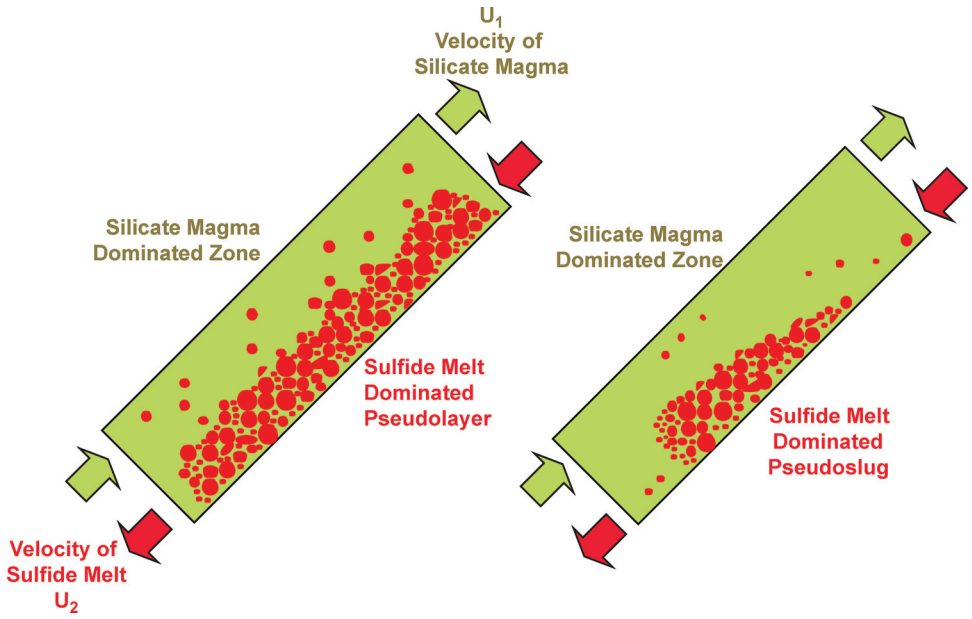

LIPs are well exposed in multiple river sections, are well studied, and calculated magma to sulfide ratios (*R* factors) for related mineralization are commonly in the range 100–1100, so not an insignificant amount of magma/lava, and yet none contain sulfides.

(3) Transported sulfide droplets may have dissolved by mixing sulfide-saturated, metal-depleted, ore-forming magmas with later sulfide-undersaturated, metal-undepleted magmas. This occurred at Kambalda because the S source was thin and was eventually completely eroded upstream, so uncontaminated lavas in the channel flow facies flushed out any evidence of contamination or metal depletion (Barnes et al. 2013; Lesher and Arndt 1995; Lesher et al. 2001). If the magma flux after ore deposition was similar to that during ore formation, which is consistent with the large amount of overlying in situ crystallized olivine accumulation (Lesher 1989), the dilution factor can be estimated to be 6000–30 000 using the magma to sulfide ratios calculated from PGE contents (100–500: Lesher and Campbell 1993) and the olivine cumulate to sulfide ratio in the host units (average 60:1: Lesher et al. 1981). This level of dilution in downstream lavas would dissolve any suspended sulfides and erase any metal depletion signature. However, systems that had access to thicker S sources, as at Perseverance, Raglan, and Thompson (Lesher et al. 2001), as well as at Duluth, Norilsk, Pechenga, remained sulfide saturated during the replenishment process and contain ubiquitous sulfides in the overlying host unit. Thus, even if the magma fluxes were similar, the downstream (upsystem) equivalents of these should also contain sulfides.

(4) Sulfide droplets may have been lost due to degassing. This is possible, but Fe–Ni–Co–Cu–PPGE and especially IPGE are much less volatile than S (Lodders 2003), so even if S were lost, the lavas would contain anomalous abundances of chalcophile elements. Because sulfide/silicate partition coefficients for the PGE are so high (up to 10^6: Mungall and Brenan 2003), a magma containing only 0.1% sulfide droplets that formed at magma to sulfide ratios (*R* factors) of 1000, 10 000, and 100 000 (spanning the range for Norilsk) from a magma originally containing 10 ppb Pd would end up containing 20, 110, or 920 ppb Pd, respectively, if degassed (Fig. 7). A magma that had been strongly depleted in PGE >>> Cu > Ni > Co via exchange with sulfide (e.g., Nadezhdinsky basalts at Norilsk: Brügmann et al. 1993) could theoretically have carried some sulfide droplets, degassed, and retained low metal contents (S.J. Barnes, personal commnication, 2018), but the fact remains that no enrichments of any significant magnitudes have been reported in the extrusive components of LIPs (e.g., Arndt et al. 2005; Day et al. 2013; Zhang et al. 2008), except where they contain mineralization generated at that level (e.g., Fiorentini et al. 2010; Lesher et al. 2001).

(5) There may have been surfactants present in nature that lowered the interfacial tension of sulfide droplets, allowing them to coalesce more readily than predicted from experiments in surfactant-free (Mungall and Su 2005; Su et al. 2005) and analog (De Bremond d'Ars et al. 2001) experiments, facilitating downward countercurrent flow. Many of magmas that formed magmatic Ni–Cu–PGE deposits interacted with their wall rocks, some of which were unconsolidated (e.g., Alexo–Dundonald, Kambalda, Perseverance, and Raglan) or semiconsolidated (e.g., Duluth) and contained saline to hypersaline and sometimes carbonaceous fluids that may have modified interfacial tensions. Others (e.g., Norilsk) may have produced similar fluids when devolatilized.

(6) As discussed above, sulfides may have settled as slugs (domains of sulfide melt larger than droplets or globules), "pseudoslugs" (hydrodynamically coherent domains containing both sulfide and silicate melts), or slurries/pseudolayers (layers containing both sulfide and silicate melts) as suggested by Arndt et al. (2013), Barnes et al. (2016), Barnes and Robertson (2019), and Lesher (2013, 2017).

There are obviously conditions of very high velocity and turbulence where sulfides could be transported upward, but the absence of sulfide droplets in the volcanic sequences overlying mineralized intrusions that are almost universally interpreted as open systems indicates that these conditions are rarely, if ever, achieved.

The difficulty of transporting sulfides vertically explains why Ni–Cu–PGE deposits are so rare in the subvertical parts of magmatic systems. An exception is Voisey's Bay where sulfides are present in some of the subvertical parts of the system (e.g., Evans-Lamswood et al. 2000), but this is not common and may reflect the high effective viscosity of a system containing abundant xenoliths. Considering the density relationships, it is equally

Fig. 9. Schematic longitudinal sections (not to scale) through dynamic (flow-through) (A) volcanic and (B) intrusive conduits (bladed dikes, chonoliths, channels, and channel-flow facies of sheet flows/sills) involving thermomechanical erosion of S-rich horizons, generation of sulfide xenomelts ± xenoliths ± silicate xenomelts ± xenovolatiles, dynamic upgrading of metal tenors in sulfide xenomelts, and localization in embayments. Modified from Lesher (2017), Lesher et al. (2001), and Lesher and Keays (2002). [Colour online.]

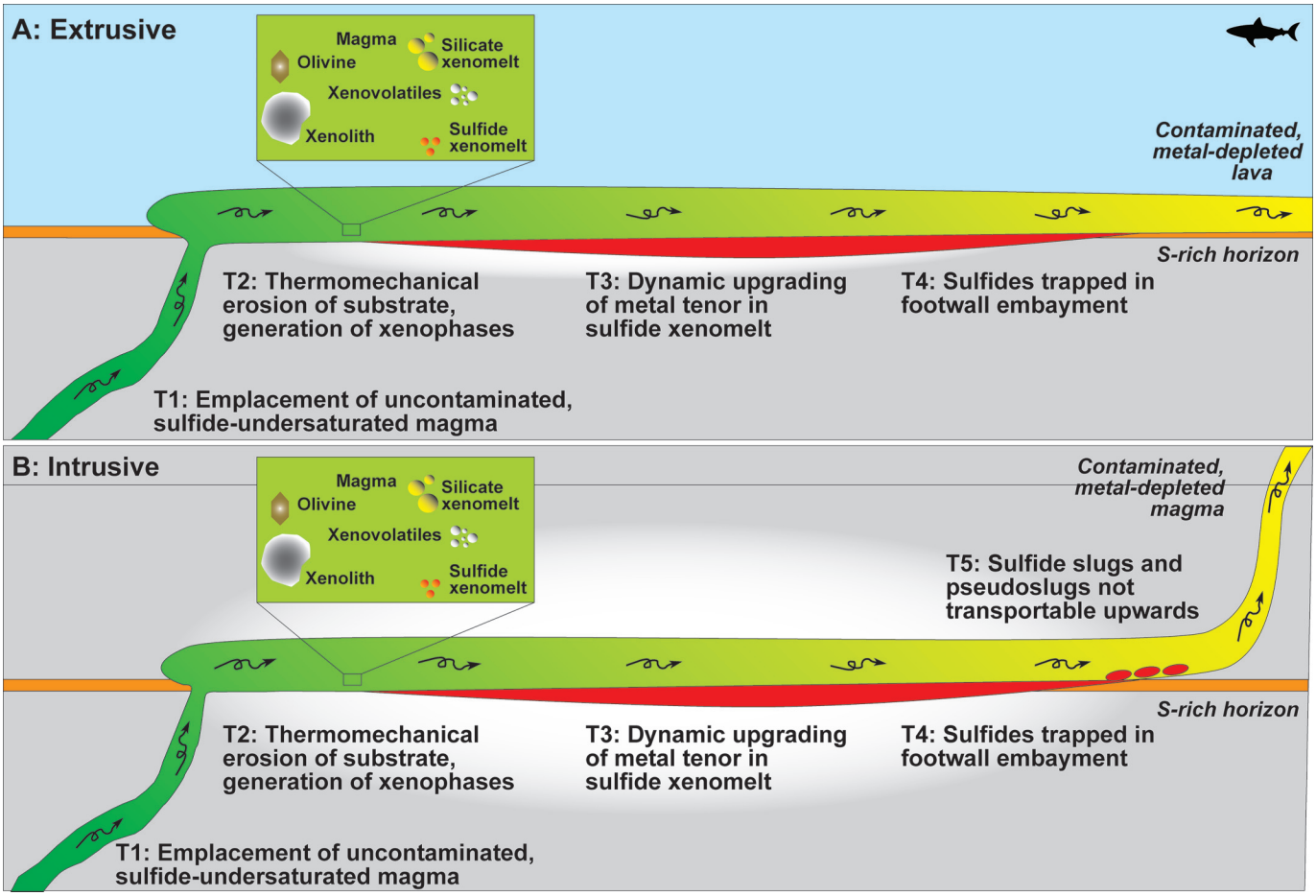

likely that sulfides flowed downwards/backwards (Arndt et al. 2013; Barnes et al. 2016; Lesher 2013, 2017) rather than upwards.

If sulfides were less vertically transportable than commonly assumed, this means that most sulfides formed at or above the stratigraphic level where they are found. This is consistent with the evidence in most deposits for incorporation of S from nearby sources (Table 1).

Ore genesis

Our understanding of the details of the ore formation process is incomplete, as we see only a snapshot at the end, which rarely preserves the dynamic conditions that occurred during ore formation. However, devolatilization of S from country rocks (e.g., Naldrett 1966; Ripley and Al-Jassar 1987) can be precluded because that process is too slow (Robertson et al. 2015*a*). Wholesale assimilation of S-bearing country rocks (Lesher et al. 1984; Mainwaring and Naldrett 1977) can be precluded because magmas cannot dissolve and reprecipitate that much sulfide (Lesher and Campbell 1993). As discussed above, physical transport of sulfides from the mantle (Barnes and Robertson 2019), exsolution of sulfides from the magma or incorporation of S during ascent (e.g., Arndt et al. 2003; Barnes et al. 2016; Barnes and Robertson 2019; De Waal et al. 2004; Lesher et al. 1981; Lightfoot and Evans-Lamswood 2015; Lightfoot et al. 2012; Naldrett 2011), or transport from "staging chambers" (e.g., Lightfoot and Keays 2005; Song et al. 2008; Song et al. 2006) is also unlikely.

A model that best fits available data involves (1) thermomechanical erosion of S-bearing substrates (e.g., Huppert et al. 1984; Lesher et al. 1984) in subhorizontal magma/lava conduits, (2) buoyant rise of molten footwall that is normally assimilated into the silicate magma and only rarely preserved in flanking sheet facies (e.g., Lesher and Arndt 1995) or ore pinchouts (e.g., Staude et al. 2017), and (3) horizonal or downward transport and upgrading of sulfides during transport along the conduit (e.g., Lesher and Burnham 2001; Lesher and Campbell 1993) until a suitable fluid dynamic trap is reached or the flow rate declines (Fig. 9).

The relatively low magma to sulfide ratios (<1100) in most deposits suggest that the sulfides were transported relatively short distances in suspension or longer distances as a dense segregated lower layer (see below). Norilsk is an exception, with magma to sulfide ratios up to 10 000 for massive and semimassive ores and up to 100 000 for disseminated ores (Naldrett 2004), which must have formed in a particularly dynamic and (or) long-lasting system, possibly because rising magmas were trapped by and focused along a stratigraphic interval between low-density coals and anhydrites and accumulating flood basalts.

Direct measurements and numerical models indicate that the rate of thermomechanical erosion below a turbulently flowing mafic–ultramafic lava channel is much greater than the rate of heat conduction into the rocks, which means that during the ore-forming process, the rock would have melted over a very narrow but rapidly moving interval (1–100 m/day, depending on the

Fig. 10. Schematic cross-section of a laterally extensive mafic intrusive complex in a sedimentary basin (modified from Magee et al. 2016) and overlying flood basalts. 1, Mineralized lava channels, channelized flows/sills, bladed dikes, and chonoliths flowing over/along S-bearing horizons; 2, barren lava channels, channelized flows/sills, bladed dikes, and chonoliths flowing over/along S-poor horizons; 3, barren unchannelized sheet flows/sills/dikes flowing over/along S-bearing or S-poor horizons. [Colour online.]

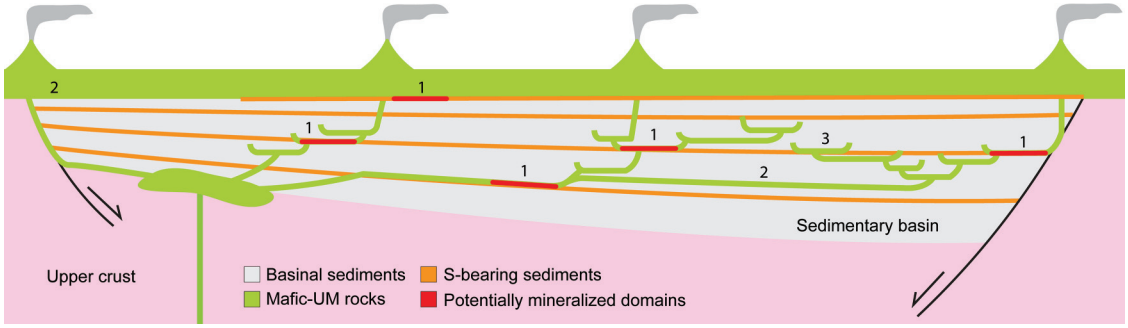

thickness and physical–thermal characteristics of the lava/magma conduit and the textural–physical–thermal characteristics of the country rock) (e.g., Huppert and Sparks 1985; Kauahikaua et al. 1998; Williams et al. 1998, 2011, 2001). There are no direct measurements for intrusions and numerical models for erosion by invasive (downward burrowing) lava channels (e.g., Cataldo et al. 2017) and ore-forming intrusions are still being developed, but with all else equal, cooling rates should be slower and erosion rates should be faster.

Ore localization

In many cases, there is direct evidence for incorporation of S from the local country rocks (see Lesher and Groves 1986; Lesher 2017; Lesher and Burnham 2001), but as noted above, in most localities, sulfide melts must be incorporated from along strike or higher in the system and must be transported to the site of localization.

In some cases, extrusive deposits occur in vents or proximal to their eruptive sites (see Groves et al. 1984; Lesher 1989; Page and Schmulian 1981; Perring 2015; Viljoen et al. 1976). However, most of these deposits are distal (10s to 100s km) from their eruptive sites (Groves et al. 1984; Lesher 1989, 2007; Lesher et al. 1984). The sills and dikes in LIPs extend for distances 10–100 times their height (Townsend et al. 2017), as far or farther than the lavas (up to 2500 km in the case of the Siberian Traps: Malich et al. 1974). So, even if the deposits at Norilsk occur near the main magmatic centre (Naldrett 1992), sills farther from the centre were also likely fed from central conduits (see e.g., Magee et al. 2016) and if channelized and intruded along the same or similar S-rich parts of the sedimentary basin may also host Ni–Cu–PGE mineralization (Fig. 10).

Nondynamic sheet sills or dikes will not be able to generate significant amounts of mineralization even if they intersect a S-bearing horizon. Lava channels, channelized sheet flow/sills, chonoliths, and bladed-shaped dikes will be able to generate significant amounts of mineralization only if they intersect a S-bearing horizon (Fig. 10).

With all else equal, concordant bodies, lava channels flowing across S-bearing substrates (as at Alexo, Kambalda, and Raglan) and channelized sills (as at Norilsk, Pechenga, and Thompson), chonoliths, or bladed dikes (as at Eagle's Nest and Expo-Méquillon) intruding along a S-bearing unit, will be able to access greater amounts of crustal S than discordant bodies (Fig. 10). Similarly, a subhorizontal unit will be able to retain sulfides better than a subvertical unit. This does not mean that the host unit must be perfectly concordant and subhorizontal at the time of emplacement but that is clearly a more favourable scenario.

The Ni–Cu–PGE mineralization in LIPs occurs in several locations within the host units depending on how and when it formed (Lesher 1989; Lesher and Keays 2002).

Type I stratiform basal mineralization occurs as massive ± semimassive ± net-textured ± disseminated mineralization at or near the basal contact of the host unit, indicating that the sulfides were emplaced at an early stage in the crystallization of the host unit. Examples include Alexo, Kambalda, Perseverance, Norilsk, Raglan, Sudbury, and parts of Jinchuan and Voisey's Bay. Mineralization is typically but not always localized in embayments in the footwall rocks. The embayments localizing extrusive deposits (including Sudbury) appear to be generated by thermomechanical erosion (e.g., Duuring et al. 2010; Houlé et al. 2012; Lesher 2007) or to be preexisting topographic features that have been variably modified by thermomechanical erosion and (or) deformation (e.g., Gregory 2005; Lesher 1989; Lesher and Barnes 2009; Staude et al. 2017). The ore-localizing features in intrusive deposits have been less well studied but are logically structural and (or) thermomechanically erosional features. In both environments, the embayments are fluid-dynamic traps for sulfides transported subhorizontally or downwards via countercurrent flow, as argued above. In many cases, Type I massive sulfides have infiltrated footwall rocks to varying degrees (e.g., most deposits at Kambalda and Raglan, Norilsk, Sudbury, and Uitkomst) and more rarely hanging-wall rocks (e.g., Cu-rich hanging-wall ores above the Kharealakh intrusion at Norilsk). As noted previously, this can be attributed to the lower solidification temperature of sulfides relative to silicates.

Type II strata-bound internal mineralization occurs as zones or layers, typically of fine to coarse disseminations but sometimes net-textured or massive layers, within the central parts of the host unit, indicating that the sulfides were emplaced at an intermediate stage in the crystallization of the host unit. Examples include Dumont, Mt Keith, and Mirabela and parts of Jinchuan, Kambalda, and Norilsk. The accumulations of sulfides suspended in the throats of what appear in cross section to be subvertical funnels (e.g., Eagle, Tamarack, Kalatongke, Huangshan, Huangshandong, and Qingkuangshan) also fall into this category but pose a special problem for models involving emplacement from below. However, this can be explained if the "funnels" are not feeders with magma coming up from underneath, but if they represent the lower parts of subhorizontal blade-shaped dikes or chonoliths, as suggested by Mungall (2007), Barnes and Mungall (2018), and Lu et al. (2019), in which magma flow was subhorizontal.

Type III stratiform internal "reef" style mineralization occurs as layers or zones of very finely disseminated sulfides within the host units. In these cases (e.g., Bushveld Merensky Reef, Sillwater JM Reef, and Skaergaard Platinova Reef), the amounts of sulfide are so small that they can be dissolved in the magma and precipitate by any of the many mechanisms that have been proposed to generate these deposits (e.g., Cawthorn et al. 2005).

These mineralization types, and magmatic–diffusional, magmatic–hydrothermal, and tectonically mobilized variations described by

Table 3. Physical properties of komatiites, komatiitic basalts, and flood basalts (Arndt et al. 2008; Huppert and Sparks 1985; Williams et al. 2011).

	Komatiite	Komatiitic basalt	Tholeiitic basalt
Liquidus temperature (°C)	1600	1420	1160
Solidus temperature (°C)	1200	1150	1080
Crystallization interval (°C)	400	270	80
Slope of liquidus (°C/% crystallization)	4	2.7	0.8
Specific heat ($J \cdot kg^{-1} \cdot °C^{-1}$)	730	1640	1480
Dynamic viscosity at liquidus (Pa s)	0.13	0.74	39
Density at liquidus (kg/m^3)	2800	2800	2750

(Lesher and Keays 2002), are not mutually exclusive. Some bodies contain only Type I (e.g., Sudbury) and have just a single S source, normally the local footwall rocks. Some bodies contain Types I and II (e.g., Kambalda, Kevitsa, Perseverance, and Raglan) and may have accessed the same S source(s) during multiple stages of formation of the host body. Some contain Types I and III (e.g., Bushveld, Duluth, and Stillwater) and had multiple S sources (e.g., footwall rocks and the magma).

Maier et al. (2001) attributed a paucity of significant Ni–Cu–PGE mineralization in large layered intrusions to the greater ability of magmas focused in conduits to entrain, transport, and upgrade sulfides. Some layered intrusions contain significant *amounts* of Ni–Cu–PGE sulfides (e.g., Platreef and Flatreef in the Bushveld Complex, Duluth, Kevitsa, Mirabela, Stillwater) but the *grades* are typically lower than in magma/lava channels. The amounts of sulfide that accumulate during magma replenishments in large layered intrusions (e.g., Bushveld Merensky Reef and Stillwater JM Reef) are typically very small, consistent with the point made above that the magmas that feed LIPs do not carry sulfides. The only place where significant amounts of sulfide have formed in layered intrusions is along contact zones (e.g., Bushveld Platreef and Flatreef, River Valley, and Stillwater) or in their feeders (e.g., Uitkomst). Thus, the point made by Maier et al. (2001) is valid, but a more complete explanation within the context of this discussion is that large layered intrusions lacked the focused flow that enabled the magma to incorporate significant amounts of S from country rocks and to generate high-grade ores.

If sulfides are preferentially localized in the subhorizontal parts of mineralized systems and if magmatic systems feeding LIPs are dominated by subhorizontal components (Magee et al. 2016), this suggests much more horizontal transport (Fig. 10) and much less upward transport than emphasized in many models (e.g., Arndt et al. 2003; Barnes et al. 2016; Barnes and Robertson 2019; De Waal et al. 2004; Lightfoot and Evans-Lamswood 2015; Lightfoot and Keays 2005; Lightfoot et al. 2012; Naldrett 2011; Song et al. 2008; Song et al. 2006).

Secular trends in volcanic/subvolcanic setting

The changes in volcanic/subvolcanic settings through time reflect changes in the compositions of the magmas through time.

(1) Komatiites and komatiitic basalts had higher liquidus temperatures, larger intervals between the liquidus and solidus, steeper liquidus surfaces, and lower viscosities (Table 3), so were able to form highly channelized flows, chonoliths, and sills that were capable of thermomechanically eroding and incorporating S from underlying rocks (Huppert and Sparks 1985; Lesher et al. 1984; Williams et al. 1998).
(2) Basalts had lower liquidus temperatures, narrower intervals between the liquidus and solidus, shallower liquidus surfaces, and higher viscosities (Table 3), so were less able to form channelized flows that were capable of thermomechanically eroding and incorporating S from underlying rocks. There are examples of lava channels/tubes on shield volcanoes that eroded their substrates (e.g., Kauahikaua et al. 1998; Williams et al. 2004), but most flood basalts were emplaced as lava lobes (Self et al. 2014) that were not sufficiently channelized to thermomechanically erode their substrates.

The intrusions where we find Ni–Cu–PGE deposits, including those associated with basaltic and picritic magmas, were channelized, but not because they were hot or had low viscosity but because (1) magma fluxes were sufficiently high and (2) they were emplaced under physical conditions (overburden density, country rock rheology, regional tectonic stresses, etc.) (e.g., Kavanagh et al. 2017; Muirhead et al. 2014; Thomson 2007) that favoured the formation of horizontal magma conduits (blade-shaped dikes, chonoliths, channelized sills, channel-flow facies of sheet sills, and lava channels) rather than sheet dikes and sheet sills.

Differential endowment

Most LIPs contain little or no known Ni–Cu–PGE mineralization (e.g., ~17 Ma Columbia River, ~31–25 Ma Ethiopia–Yemen, ~66 Ma Deccan, ~95 Ma Caribbean, 180 Ma Ferrar, ~130–60 Ma High Artic, ~120–95 Ma Kerguelen, ~122–90 Ma Ontong Java ~130 Ma Paraná-Etendeka, and ~511 Ma Kalkarinji) and are not listed in Table 1. There are three possible reasons for this.

(1) *Poor channelization*: Some do not contain known intrusions other than thin feeder dikes (Ernst 2014), so may not have contained any magma conduits capable of thermomechanically eroding significant amounts of S-bearing country rocks.
(2) *S-poor country rocks*: Some may have been channelized but lacked access to significant amounts of crustal S. Most LIP compilations do not indicate whether S-rich country rocks are present in the system.
(3) *Unexposed mineralized intrusive components*: The CAMP and Kalkarinji LIPs, for example, contain intrusions into evaporites (Svensen et al. 2018) and may well be mineralized.

Although not all LIPs have been explored to the same degree, some (e.g., Norseman–Wiluna Belt of Western Australia, Bird River – Uchi – Oxford-Stull – La Grande – Eastmain domain of Superior Province, Circum–Superior Belt, and Siberian Trap) appear to contain much more mineralization than others (e.g., Brazil, Karoo, southern Superior, and Zimbabwe) and some LIPs (e.g., Circum–Superior Belt) are well mineralized in some areas (Cape Smith and Thompson Belts) and less well mineralized in other areas (Labrador Trough) and apparently nonmineralized in some areas (Fox River Belt and Sutton Inlier). These can probably be attributed to four factors.

(1) *Differences in magma flux*: Differences in the density/rheology of the crust or magma access may have controlled magma flux and the ability to thermomechanically erode S-bearing country rocks.
(2) *Differences in degree of channelization*: The stress regime and rheology of the country rocks may have controlled the degree of channelization and whether the magmas were emplaced as sheet sills or sheet dikes (less favourable) or as channelized sills, chonoliths, or blade-shaped dikes (more favourable).

(3) *Differences in access to crustal S*: Different systems contain different amounts of S at the levels of emplacement. The best scenario is where a channelized lava flows across a S-rich substrate or where a horizontal magma conduit (channelized sill, chonolith, or blade-shaped dike) is emplaced at the same stratigraphic level as a S-rich country rock (Figs. 9 and 10).
(4) *Differences in exposure*: Most Archean and Proterozoic LIPs are deformed and eroded, exposing potentially mineralized lavas and intrusions, whereas most Phanerozoic LIPs are undeformed and only partly eroded, hiding potentially mineralized lavas and intrusions.

The best deposits form where the first three are favourable (Fig. 10). For example, highly channelized lavas at Kambalda, Perseverance, and Raglan were preferentially emplaced onto S-rich substrates (Lesher 2007; Lesher et al. 1984), channelized sills at Pechenga were preferentially emplaced into S-rich pelites (Barnes et al. 2001), channelized sills in the Thompson Nickel Belt were preferentially emplaced into sulfide–facies iron formations (Layton-Matthews et al. 2010), and channelized sills at Norilsk were preferentially emplaced into a sequence containing evaporites and coal (Naldrett 2004).

However, there is a critical balance between the size of the system, the degree of channelization, and the amount of S (see discussion by Lesher et al. 2001). Too much magma and too little external S and the magma will be able to dissolve most or all of the S, resulting in mainly disseminated mineralization (e.g., Duluth, Dumont, and Mt Keith). Too much external S and too little magma and there will be excess sulfide, resulting in relatively low-tenor mineralization (especially in terms of PGE contents) (e.g., Thompson and Voisey's Bay). Better balances between the amount of magma and S result in both large tonnages and high grades (e.g., Kambalda, Norilsk, Pechenga, and Raglan).

Conclusions

(1) The age, composition of the mantle source, degree of partial melting, and degree of crustal contamination and precise tectonic setting (continental rift versus rifted continental margin versus trans-tensional) do not appear to be important controls on the genesis of magmatic Ni–Cu–PGE deposits. The most important genetic controls appear to be lava/magma channelization and density/rheologically controlled access to crustal S.
(2) Molten Fe–Ni–Cu–PGE sulfides in LIPS are unlikely to have been transported upward for significant distances but may have flowed backward in some cases and were likely transported horizontally for significant distances in some cases.
(3) Most magmatic Fe–Ni–Cu–PGE sulfide melts likely formed at or above the stratigraphic levels where they are found. The stratigraphic level of emplacement is not particularly important, although many of the largest deposits are volcanic or subvolcanic and fewer are plutonic.
(4) The precise morphology of the host unit (lava channel versus channelized sheet flow and blade-shaped dike versus chonolith versus channelized sill) is not particularly important, although the highest grade deposits appear to be hosted by lava/magma channels and channelized flows/sills.
(5) The orientation of the host unit appears to be very important: most deposits are hosted by bodies or segments of bodies that were originally subhorizontal and more-or-less concordant to stratigraphy.

Acknowledgements

This research has been supported by grants from the Natural Sciences and Engineering Council of Canada (Discovery Grant No. 203171-1212) and the Canada First Research Excellence Fund. I am grateful to Marie-Claude Williamson for inviting me to contribute to this special issue, to Nick Arndt, Steve Barnes, Michel Houlé, Jim Mungall, and Benoit Saumur for stimulating discussions on sulfide transport, and to Steve Barnes and an anonymous CJES reviewer for insightful reviews of the manuscript. This is Mineral Exploration Research Centre Metal Earth Contribution No. MERC-ME-2019-120.

References

Ariskin, A.A., Kislov, E.V., Danyushevsky, L.V., Nikolaev, G.S., Fiorentini, M.L., Gilbert, S., et al. 2016. Cu–Ni–PGE fertility of the Yoko–Dovyren layered massif (northern Transbaikalia, Russia); thermodynamic modeling of sulfide compositions in low mineralized dunite based on quantitative sulfide mineralogy. Mineralium Deposita, **51**(8): 993–1011. doi:10.1007/s00126-016-0666-8.

Arndt, N.T., Czamanske, G.K., Walker, R.J., Chauvel, C., and Fedorenko, V.A. 2003. Geochemistry and origin of the intrusive hosts of the Noril'sk–Talnakh Cu–Ni–PGE sulfide deposits. Economic Geology, **98**: 495–515. doi:10.2113/gsecongeo.98.3.495.

Arndt, N.T., Lesher, C.M., and Czamanske, G.K. 2005. Mantle-derived magmas and magmatic Ni–Cu–PGE deposits. *In* Economic geology. One hundredth aniversary volume. Society of Economic Geologists, Inc., Littleton, Co. pp. 5–24.

Arndt, N.T., Lesher, C.M., and Barnes, S.J. 2008. Komatiite. Cambridge University Press, Cambridge. 488 pp.

Arndt, N.T., Barnes, S.J., Robertston, J., Lesher, C.M., and Cruden, S. 2013. Downward injection of sulfide slurries; their role in the formation of Ni sulfide deposits. Mineralogical Magazine, **77**(5): 618. doi:10.1180/minmag.2013.077.5.1.

Barnes, S.J. 2006. Komatiite-hosted nickel sulfide deposits: geology, geochemistry, and genesis. Society of Economic Geologists Special Publication **13**: 51–118.

Barnes, S.J., and Fiorentini, M.L. 2012. Komatiite magmas and sulfide nickel deposits: a comparison of variably endowed archean terranes. Economic Geology, **107**(5): 755–780. doi:10.2113/econgeo.107.5.755.

Barnes, S.J., and Mungall, J.E. 2018. Blade-shaped dikes and nickel sulfide deposits: a model for the emplacement of ore-bearing small intrusions. Economic Geology, **113**(3): 789–798. doi:10.5382/econgeo.2018.4571.

Barnes, S.J., and Robertson, J.C. 2019. Time scales and length scales in magma flow pathways and the origin of magmatic Ni–Cu–PGE ore deposits. Geoscience Frontiers, **10**(1): 77–87. doi:10.1016/j.gsf.2018.02.006.

Barnes, S.J., Heggie, G.J., and Fiorentini, M.L. 2013. Spatial variation in platinum group element concentrations in ore-bearing komatiite at the Long–Victor deposit, Kambalda Dome, Western Australia: enlarging the footprint of nickel sulfide orebodies. Economic Geology, **108**(5): 913–933. doi:10.2113/econgeo.108.5.913.

Barnes, S.J., Cruden, A.R., Arndt, N., and Saumur, B.M. 2016. The mineral system approach applied to magmatic Ni–Cu–PGE sulphide deposits. Ore Geology Reviews, **76**: 296–316. doi:10.1016/j.oregeorev.2015.06.012.

Barnes, S.J., le Vaillant, M., Godel, B., and Lesher, C.M. 2019. Droplets and bubbles: solidification of sulphide-rich vapour-saturated orthocumulates in the Norilsk–Talnakh Ni–Cu–PGE ore-bearing intrusions. Journal of Petrology, **60**: 269–300. doi:10.1093/petrology/egy114.

Barnes, S.-J., and Lightfoot, P.C. 2005. Formation of magmatic nickel sulfide deposits and processes affecting their copper and platinum group element contents. *In* Economic geology. One hundredth anniversary volume. Society of Economic Geologists, Inc., Littleton, Co. pp. 179–214.

Barnes, S.-J., Melezhik, V.A., and Sokolov, S.V. 2001. The composition and mode of formation of the Pechenga nickel deposits, Kola Peninsula, northwestern Russia. The Canadian Mineralogist, **39**: 447–471. doi:10.2113/gscanmin.39.2.447.

Bekker, A., Barley, M.E., Fiorentini, M.L., Rouxel, O.J., Rumble, D., and Beresford, S.W. 2009. Atmospheric sulfur in Archean komatiite-hosted nickel deposits. Science, **326**(5956): 1086–1089. doi:10.1126/science.1177742. PMID: 19965423.

Branquet, Y., Gumiaux, C., Sizaret, S., Barbanson, L., Wang, B., Cluzel, D., et al. 2012. Synkinematic mafic/ultramafic sheeted intrusions: emplacement mechanism and strain restoration of the Permian Huangshan Ni–Cu ore belt (eastern Tian Shan, NW China). Journal of Asian Earth Sciences, **56**: 240–257. doi:10.1016/j.jseaes.2012.05.021.

Brügmann, G.E., Naldrett, A.J., Asif, M., Lightfoot, P.C., Gorbachev, N.S., and Fedorenko, V.A. 1993. Siderophile and chalcophile metals as tracers of the evolution of the Siberian Trap in the Noril'sk region, Russia. Geochimica et Cosmochimica Acta, **57**: 2001–2018. doi:10.1016/0016-7037(93)90089-F.

Bryan, S.E., and Ernst, R.E. 2008. Revised definition of large igneous provinces (LIPs). Earth-Science Reviews, **86**(1–4): 175–202. doi:10.1016/j.earscirev.2007.08.008.

Burgess, S.D., and Bowring, S.A. 2015. High-precision geochronology confirms voluminous magmatism before, during, and after Earth's most severe extinction. Science Advances, **1**(7): 1–14. doi:10.1126/sciadv.1500470.

Callegaro, S., Marzoli, A., Bertrand, H., Blichert-Toft, J., Reisberg, L., Cavazzini, G., et al. 2017. Geochemical constraints provided by the Freetown Layered Complex (Sierra Leone) on the origin of high-Ti tholeiitic CAMP magmas. Journal of Petrology, **58**(9): 1811–1840. doi:10.1093/petrology/egx073.

Campbell, I.H., and Griffiths, R.W. 1990. Implications of mantle plume structure

for the evolution of flood basalts. Earth and Planetary Science Letters, **99**: 79–93. doi:10.1016/0012-821X(90)90072-6.

Campbell, I.H., and Griffiths, R.W. 1992. The changing nature of mantle hotspots through time: implications for the chemical evolution of the mantle. Journal of Geology, **92**: 497–523.

Campbell, I.H., and Griffiths, R.W. 2014. Did the formation of D″ cause the Archaean–Proterozoic transition? Earth and Planetary Science Letters, **388**: 1–8. doi:10.1016/j.epsl.2013.11.048.

Cataldo, V., Williams, D.A., Schmeeckle, M.W., Lesher, C.M., and Clarke, A.B. 2017. Building a 3-D model of thermal erosion by turbulent lava at Raglan, Cape Smith Belt, New Québec, Canada. 48th Lunar and Planetary Science Conference, The Woodlands, Texas, 20–24 March, 2017.

Cawthorn, R.G., Barnes, S.J., Ballhaus, C., and Malich, K.N. 2005. Platinum group element, chromium and vanadium deposits in mafic and ultramafic rocks. *In* Economic geology. One hundredth anniversary volume. Society of Economic Geologists, Inc., Littleton, Co. pp. 215–249.

Chalokwu, C.I., Armitage, A.E., Seney, P.J., Wurie, C.A., and Bersch, M. 1995. Petrology of the Freetown Layered Complex, Sierra Leone: Part I. Stratigraphy and mineral–chemical evidence for multiple magma injection. International Geology Review, **37**: 230–253. doi:10.1080/00206819509465402.

Cruden, A.R., Burrows, D.R., and Evans-Lamswood, D. 2000. Structural, tectonic and fluid mechanical controls on emplacement of the Voisey's Bay troctolite and its Ni–Cu–Co mineralisation. Program with Abstracts. Geological Association of Canada – Mineralogical Association of Canada Joint Annual Meeting **25**.

Czamanske, G.K., Wooden, J.L., Zientek, M.L., Fedorenko, V.A., Zen'ko, T.E., Kent, J., et al. 1994. Geochemical and isotopic constraints on the petrogenesis of the Noril'sk–Talnakh ore-forming system. Ontario Geological Survey Special Volume, **5**: 313–341.

Czamanske, G.K., Zen'ko, K.E., Fedorenko, V., Calk, L.C., Budahn, J.R., Bullock, J.H.J., et al. 1995. Petrographic and geochemical characterization of ore-bearing intrusions of the Noril'sk Type, Siberia: with discussion of their origin. Resource Geology Special Issue, **18**: 1–48.

Day, J.M.D., Pearson, D.G., and Hulbert, L.J. 2013. Highly siderophile element behaviour during flood basalt genesis and evidence for melts from intrusive chromitite formation in the Mackenzie large igneous province. Lithos (Oslo), **182–183**: 242–258. doi:10.1016/j.lithos.2013.10.011.

De Angelis, M., Hoyle, M.W.H., Peters, W.S., and Wightman, D. 1987. The nickel–copper deposit at Radio Hill, Karratha, Western Australia. Australasian Institute Mining Metallurgy Bulletin and Proceedings, **292**: 61–74.

De Bremond d'Ars, J., Arndt, N.T., and Hallot, E. 2001. Analog experimental insights into the formation of magmatic sulfide deposits. Earth and Planetary Science Letters, **186**: 371–381. doi:10.1016/S0012-821X(01)00254-0.

De Waal, S.A., Xu, Z.G., Li, C.S., and Mouri, H. 2004. Emplacement of viscous mushes in the Jinchuan Ultramafic intrusion, western China. The Canadian Mineralogist, **42**: 371–392. doi:10.2113/gscanmin.42.2.371.

Ding, X., Ripley, E.M., and Li, C. 2012*a*. PGE geochemistry of the Eagle Ni–Cu–(PGE) deposit, upper Michigan: constraints on ore genesis in a dynamic magma conduit. Mineralium Deposita, **47**(1–2): 89–104. doi:10.1007/s00126-011-0350-y.

Ding, X., Ripley, E.M., Shirey, S.B., and Li, C. 2012*b*. Os, Nd, O and S isotope constraints on country rock contamination in the conduit-related Eagle Cu—Ni–(PGE) deposit, Midcontinent Rift System, upper Michigan. Geochimica et Cosmochimica Acta, **89**: 10–30. doi:10.1016/j.gca.2012.04.029.

Dobrovinski, I.E., Esin, O.A., Barmin, L.N., and Chuchmarev, S.K. 1969. Physicochemical properties of sulphide melts. Russian Journal of Physical Chemistry, **43**: 1769–1771.

Dobson, D.P., Crichton, W.A., Vocadlo, L., Jones, A.P., Wang, Y., Uchida, T., et al. 2000. In situ measurement of viscosity of liquids in the Fe–FeS system at high pressures and temperatures. American Mineralogist, **85**(11–12): 1838–1842. doi:10.2138/am-2000-11-1231.

Duuring, P., Bleeker, W., Beresford, S.W., and Hayward, N. 2010. Towards a volcanic–structural balance: relative importance of volcanism, folding, and remobilisation of nickel sulphides at the Perseverance Ni–Cu–(PGE) deposit, Western Australia. Mineralium Deposita, **45**(3): 281–311. doi:10.1007/s00126-009-0274-y.

Eckstrand, R.O., and Williamson, B.L. 1985. Vesicles in the Dundonald komatiites. Program and abstracts. Geological Association of Canada – Mineralogical Association of Canada joint annual meeting, **10**: A-16.

Ernst, R.E. 2014. Large igneous provinces. Cambridge University Press, Cambridge. 653 pp.

Ernst, R., and Jowitt, S. 2013. Large igneous provinces (LIPs) and metallogeny. *In* Special Publication Society of Economic Geologists. pp. 17–51.

Evans-Lamswood, D.M., Butt, D.P., Jackson, R.S., Lee, D.V., Muggridge, M.G., Wheeler, R.I., and Wilton, D.H.C. 2000. Physical controls associated with the distribution of sulfides in the Voisey's Bay Ni–Cu–Co deposit, Labrador. Economic Geology and the Bulletin of the Society of Economic Geologists, **95**(4): 749–769. doi:10.2113/gsecongeo.95.4.749.

Fedorenko, V.A. 1994. Evolution of magmatism as reflected in the volcanic sequence of the Noril'sk region. *Edited by* P.C. Lightfoot and A.J. Naldrett. Ontario Geological Survey, Toronto, Ont. pp. 171–184.

Fiorentini, M.L., Barnes, S.J., Lesher, C.M., Heggie, G.J., Keays, R.R., and Burnham, O.M. 2010. Platinum group element geochemistry of mineralized and nonmineralized komatiites and basalts. Economic Geology, **105**(4): 795–823. doi:10.2113/gsecongeo.105.4.795.

Frost, K.M., Woodhouse, M., and Pitkajarvi, J.T. 1998. Forrestania nickel deposits. Monograph Series. Australasian Institute of Mining and Metallurgy, **22**: 365–370.

Gregory, S.K. 2005. Geology, mineralogy, and geochemistry of transitional contact/footwall mineralization in the McCreedy East Ni–Cu–PGE deposit, Sudbury Igneous Complex. *In* Department of Earth Sciences, Laurentian University, Sudbury, Ont. 131 pp.

Groves, D.I., Lesher, C.M., and Gee, R.D. 1984. Tectonic setting of the sulphide nickel deposits of the Western Australian shield. *In* Sulphide deposits in mafic and ultramafic rocks. *Edited by* D.L. Buchanan and M.J. Jones. Institute of Mining and Metallurgy, London.

Hayes, B., Bédard, J.H., Hryciuk, M., Wing, B., Nabelek, P., MacDonald, W.D., et al. 2015. Sulfide immiscibility induced by wall-rock assimilation in a fault-guided basaltic feeder system, Franklin Large Igneous Province, Victoria Island (Arctic Canada). Economic Geology, **110**(7): 1697–1717. doi:10.2113/econgeo.110.7.1697.

Holwell, D.A., Keays, R.R., Firth, E.A., and Findlay, J. 2014. Geochemistry and mineralogy of platinum group element mineralization in the River Valley Intrusion, Ontario, Canada: a model for early-stage sulfur saturation and multistage emplacement and the implications for "contact-type" Ni–Cu–PGE sulfide mineralization. Economic Geology, **109**(3): 689–712. doi:10.2113/econgeo.109.3.689.

Houlé, M.G., and Lesher, C.M. 2011. Komatiite-associated Ni—Cu–(PGE) deposits, Abitibi greenstone belt, Superior Province, Canada. Reviews in Economic Geology, **17**: 89–121.

Houlé, M.G., Gibson, H.L., Lesher, C.M., Davis, P.C., Cas, R.A.F., Beresford, S.W., et al. 2008. Komatiitic sills and multigenerational peperite at Dundonald Beach, Abitibi Greenstone Belt, Ontario: volcanic architecture and nickel sulfide distribution. Economic Geology, **103**(6): 1269–1284. doi:10.2113/gsecongeo.103.6.1269.

Houlé, M.G., Lesher, C.M., and Davis, P.C. 2012. Thermomechanical erosion at the Alexo Mine, Abitibi greenstone belt, Ontario: implications for the genesis of komatiite-associated Ni–Cu–(PGE) mineralization. Mineralium Deposita, **47**(1–2): 105–128. doi:10.1007/s00126-011-0371-6.

Houlé, M.G., Lesher, C.M., Metsaranta, R.T., Goutier, J., McNicoll, V., and Gilbert, H.P. 2013. Temporal and spatial distribution of magmatic Ni–Cu–PGE/Cr–PGE/Fe–Ti–V deposits in the Bird River/Uchi/Oxford-Stull/La Grande–Eastmain superdomain: a new metallotect within the Superior Province. SGA, **36**: 115.

Houlé, M., Lesher, C.M., and Préfontaine, S. 2018. Physical volcanology of komatiites and Ni–Cu–(PGE) deposits of the Southern Abitibi Greenstone Belt. *In* Archean base and precious metal deposits, Southern Abitibi Greenstone Belt, Canada. *Edited by* T. Monecke, P. Mercier-Langevin, and B. Dubé. Reviews in Economic Geology. pp. 103–132.

Hughes, H.S.R., McDonald, I., Boyce, A.J., Holwell, D.A., and Kerr, A.C. 2016. Sulphide sinking in magma conduits: evidence from mafic–ultramafic plugs on Rum and the wider North Atlantic igneous province. Journal of Petrology, **57**(2): 383–416. doi:10.1093/petrology/egw010.

Hulbert, L. 1997. Geology and metalllogeny of the Kluane Mafic–Utramafic Belt, Yukon Territory, Canada: Eastern Wrangellia — a new Ni–Cu–PGE metallogenic terrane. Geological Survey of Canada. 271 pp.

Hulbert, L. 2005. Geology of the Muskox Intrusion and associated Ni + Cu occurrences. Geological Survey of Canada, Calgary, Alta. Open file 4881.

Huppert, H.E., and Sparks, R.S.J. 1985. Komatiites I: Eruption and flow. Journal of Petrology, **26**: 694–725. doi:10.1093/petrology/26.3.694.

Huppert, H.E., Sparks, R.S.J., Turner, J.S., and Arndt, N.T. 1984. Emplacement and cooling of komatiite lavas. Nature, **309**: 19–22. doi:10.1038/309019a0.

Ihlenfeld, C., and Keays, R.R. 2011. Crustal contamination and PGE mineralization in the Platreef, Bushveld Complex, South Africa: evidence for multiple contamination events and transport of magmatic sulfides. Mineralium Deposita, **46**(7): 813–832. doi:10.1007/s00126-011-0340-0.

Irvine, T.N., and Smith, C.H. 1967. The ultramafic rocks of the Muskox intrusion, Northwest Territories, Canada. *In* Ultramafic and related rocks. *Edited by* P.J. Wyllie. John Wiley & Sons, New York and London, International. pp. 38–49.

James, R.S., Easton, R.M., Peck, D.C., and Hrominchuk, J.L. 2002. The East Bull Lake intrusive suite: remnants of a similar to 2.48 Ga large igneous and metallogenic province in the Sudbury area of the Canadian Shield. Economic Geology, **97**: 1577–1606. doi:10.2113/gsecongeo.97.7.1577.

Jowitt, S.M., and Ernst, R.E. 2013. Geochemical assessment of the metallogenic potential of Proterozoic LIPs of Canada. Lithos (Oslo), **174**: 291–307. doi:10.1016/j.lithos.2012.03.026.

Karykowski, B.T., Polito, P.A., Maier, W.D., and Gutzmer, J. 2015. Origin of Cu–Ni–PGE mineralization at the Manchego Prospect, West Musgrave Province, Western Australia. Economic Geology, **110**(8): 2063–2085. doi:10.2113/econgeo.110.8.2063.

Kauahikaua, J., Cashman, K.V., Mattox, T.N., Heliker, C.C., Hon, K.A., Mangan, M.T., et al. 1998. Observations on basaltic lava streams in tubes from Kilauea Volcano, Island of Hawaii. Journal of Geophysical Research: Solid Earth, **103**: 27303–27323. doi:10.1029/97JB03576.

Kavanagh, J.L., Rogers, B.D., Boutelier, D., and Cruden, A.R. 2017. Controls on sill and dyke–sill hybrid geometry and propagation in the crust: the role of fracture toughness. Tectonophysics, **698**: 109–120. doi:10.1016/j.tecto.2016.12.027.

Keays, R., and Lightfoot, P. 2010. Crustal sulfur is required to form magmatic Ni–Cu sulfide deposits: evidence from chalcophile element signatures of Siberian and Deccan Trap basalts. Mineralium Deposita, **45**(3): 241–257. doi:10.1007/s00126-009-0271-1.

Keays, R.R., and Lightfoot, P.C. 2015. Geochemical stratigraphy of the Keweenawan Midcontinent Rift volcanic rocks with regional implications for the genesis of associated Ni, Cu, Co, and platinum group element sulfide mineralization. Economic Geology, **110**(5): 1235–1267. doi:10.2113/econgeo.110.5.1235.

Kinnaird, J.A., Hutchinson, D., Schurmann, L., Nex, P., and de Lange, R. 2005. Petrology and mineralisation of the Southern Platreef: northern limb of the Bushveld Complex, South Africa. Mineralium Deposita, **40**: 576–597. doi:10.1007/s00126-005-0023-9.

Latypov, R.M. 2002. Phase equilibria constraints on relations of ore-bearing intrusions with flood basalts in the Noril'sk region, Russia. Contributions to Mineralogy and Petrology, **143**(4): 438–449. doi:10.1007/s00410-002-0355-8.

Layton-Matthews, D., Lesher, C.M., Burnham, O.M., Liwanag, J., Halden, N.M., Hulbert, L., et al. 2007. Magmatic Ni–Cu–platinum group element deposits of the Thompson Nickel Belt. *In* Mineral deposits of Canada: a synthesis of major deposit types, district metallogeny, the evolution of geological provinces, and exploration methods. Geological Associaton of Canada Special Publication 5. *Edited by* W.D. Goodfellow. Geological Associaton of Canada, Mineral Deposits Division, Ottawa, Ont. pp. 409–432.

Layton-Matthews, D., Lesher, C.M., Burnham, O.M., Hulbert, L., Peck, D.C., Golightly, J.P., et al. 2010. Exploration for komatiite-associated Ni–Cu–(PGE) mineralization in the Thompson nickel belt, Manitoba. Special Publication Society of Economic Geologists (U.S.), **15**: 513–538.

Lehmann, J., Arndt, N., Windley, B., Zhou, M.F., Wang, C.Y., and Harris, C. 2007. Field relationships and geochemical constraints on the emplacement of the Jinchuan Intrusion and its Ni–Cu–PGE sulfide deposit, Gansu, China. Economic Geology, **102**(1): 75–94. doi:10.2113/gsecongeo.102.1.75.

Lesher, C.M. 1989. Komatiite-associated nickel sulfide deposits. *In* Ore deposition associated with magmas. *Edited by* J.A. Whitney and A.J. Naldrett. Rev. Econ. Geol. Vol. 4. Economic Geology Publishing Company, El Paso, Tex. pp. 44–101.

Lesher, C.M. 2007. Ni-Cu-PGE Deposits in the Raglan Area, Cape Smith Belt, New Québec. *In* Mineral deposits of Canada: a synthesis of major deposit types, district metallogeny, the evolution of geological provinces, and exploration methods. Geological Associaton of Canada Special Publication 5. *Edited by* W.D. Goodfellow. Geological Associaton of Canada, Mineral Deposits Division, Ottawa, Ont. pp. 351–386.

Lesher, C.M. 2013. Physical transport and localization of magmatic Fe—Ni–Cu sulfide melts. *In* Society of Economic Geologists Annual Meeting. Society of Economic Geologists, Whistler, B.C.

Lesher, C.M. 2017. Roles of xenomelts, xenoliths, xenocrysts, xenovolatiles, residues, and skarns in the genesis, transport, and localization of magmatic Fe–Ni–Cu–PGE sulfides and chromite. Ore Geology Reviews, **90**: 465–484. doi:10.1016/j.oregeorev.2017.08.008.

Lesher, C.M., and Arndt, N.T. 1995. REE and Nd isotope geochemistry, petrogenesis and volcanic evolution of contaminated komatiites at Kambalda, Western Australia. Lithos, **34**(1–3): 127–157. doi:10.1016/0024-4937(95)90017-9.

Lesher, C.M., and Barnes, S.J. 2009. Komatiite-associated Ni—Cu–(PGE) Deposits. *In* 11th International Ni—Cu–PGE Symposium. *Edited by* C. Li and E.M. Ripley. Geological Publishing House of China, Xi'an, China. pp. 27–101.

Lesher, C.M., and Burnham, O.M. 2001. Multicomponent elemental and isotopic mixing in Ni–Cu–(PGE) ores at Kambalda, Western Australia. The Canadian Mineralogist, **39**: 421–446. doi:10.2113/gscanmin.39.2.421.

Lesher, C.M., and Campbell, I.H. 1993. Geochemical and fluid dynamic modeling of compositional variations in Archean komatiite-hosted nickel sulfide ores in Western Australia. Economic Geology, **88**: 804–816. doi:10.2113/gsecongeo.88.4.804.

Lesher, C.M., and Groves, D.I. 1986. Controls on the formation of komatiite-associated nickel–copper sulfide deposits. *In* Geology and metallogeny of copper deposits. *Edited by* G.H. Friedrich. Springer Verlag, Berlin. pp. 63–90.

Lesher, C.M., and Keays, R.R. 2002. Komatiite-associated Ni–Cu–PGE deposits: geology, mineralogy, geochemistry and genesis. *In* The geology, geochemistry mineralogy and mineral beneficiation of platinum group elements. *Edited by* L.J. Cabri. Canadian Institute of Mining Metallurgy and Petroleum Special Volume 54. pp. 579–617.

Lesher, C.M., and Stone, W.E. 1996. Exploration geochemistry of komatiites. *In* Igneous trace element geochemistry applications for massive sulphide exploration. *Edited by* D.A. Wyman. Geological Association of Canada. pp. 153–204.

Lesher, C.M., Lee, R.F., Groves, D.I., Bickle, M.J., and Donaldson, M.J. 1981. Geochemistry of komatiites from Kambalda, western Australia: I. Chalcophile element depletion — a consequence of sulfide liquid separation from komatiite magmas. Economic Geology, **76**: 1714–1728. doi:10.2113/gsecongeo.76.6.1714.

Lesher, C.M., Arndt, N.T., and Groves, D.I. 1984. Genesis of komatiite-associated nickel sulphide deposits at Kambalda Western Australia: a distal volcanic model. *In* Sulphide deposits in mafic and ultramafic rocks. *Edited by* D.L. Buchanan and M.J. Jones. Institute of Mining and Metallurgy, London. pp. 70–80.

Lesher, C.M., Burnham, O.M., Keays, R.R., Barnes, S.J., and Hulbert, L. 1999. Geochemical discrimination of barren and mineralized komatiites in dynamic ore-forming magmatic systems. *Edited by* R.R. Keays, C.M. Lesher, P.C. Lightfoot, and C.E.G. Farrow. Geological Association of Canada Short Course 13. pp. 451–477.

Lesher, C.M., Burnham, O.M., Keays, R.R., Barnes, S.J., and Hulbert, L. 2001. Trace-element geochemistry and petrogenesis of barren and ore-associated komatiites. Canadian Mineralogist, **39**: 673–696. doi:10.2113/gscanmin.39.2.673.

Li, C.S., and Ripley, E.M. 2005. Empirical equations to predict the sulfur content of mafic magmas at sulfide saturation and applications to magmatic sulfide deposits. Mineralium Deposita, **40**: 218–230. doi:10.1007/s00126-005-0478-8.

Li, C., and Ripley, E.M. 2011. The giant Jinchuan Ni–Cu–(PGE) deposit: tectonic setting, magma evolution, ore genesis, and exploration implications. Reviews in Economic Geology, **17**: 163–180.

Li, C., Zhang, M., Fu, P., Qian, Z., Hu, P., and Ripley, E.M. 2012. The Kalatongke magmatic Ni–Cu deposits in the Central Asian orogenic belt, NW China: product of slab window magmatism? Mineralium Deposita, **47**(1–2): 51–67. doi:10.1007/s00126-011-0354-7.

Lightfoot, P.C. 2016. Nickel sulfide ores and impact melts: origin of the Sudbury Igneous Complex. Elsevier. 680 pp.

Lightfoot, P.C., and Evans-Lamswood, D. 2015. Structural controls on the primary distribution of mafic-ultramafic intrusions containing Ni–Cu—Co–(PGE) sulfide mineralization in the roots of large igneous provinces. Ore Geology Reviews, **64**: 354–386. doi:10.1016/j.oregeorev.2014.07.010.

Lightfoot, P.C., and Keays, R.R. 2005. Siderophile and chalcophile metal variations in flood basalts from the Siberian trap, Noril'sk region: implications for the origin of the Ni–Cu–PGE sulfide ores. Economic Geology, **100**(3): 439–462. doi:10.2113/gsecongeo.100.3.439.

Lightfoot, P.C., and Naldrett, A.J. 1983. The geology of the Tabankulu section of the Insizwa Complex, Transkei, southern Africa, with reference to the nickel sulphide potential. Transactions of the Geological Society of South Africa, **86**: 169–187.

Lightfoot, P.C., and Naldrett, A.J. 1984. Chemical variation in the Insizwa Complex, Transkei, and the nature of the parent magma. The Canadian Mineralogist, **22**: 111–123.

Lightfoot, P.C., and Naldrett, A.J. 1996. Petrology and geochemistry of the Nipissing Gabbro: exploration strategies for nickel, copper, and platinum group elements in a large igneous province. Ontario Geological Survey, Toronto, Ont. 94 pp.

Lightfoot, P.C., and Zotov, I.A. 2014. Geological relationships between the intrusions, Country Rocks, and Ni–Cu–PGE sulfides of the Kharaelakh intrusion, Noril'sk region: implications for the roles of sulfide differentiation and metasomatism in their genesis. Northwestern Geology, **47**: 1–35.

Lightfoot, P.C., Hawkesworth, C.J., Olshefsky, K., Green, T., Doherty, W., and Keays, R.R. 1997. Geochemistry of tertiary tholeiites and picrites from Qeqertarssuaq (Disko Island) and Nuussuaq, West Greenland with implications for the mineral potential of comagmatic intrusions. Contributions to Mineralogy and Petrology, **128**(2–3): 139–163. doi:10.1007/s004100050300.

Lightfoot, P.C., Keays, R.R., Evans-Lamswood, D., and Wheeler, R. 2012. S saturation history of Nain plutonic suite mafic intrusions: origin of the Voisey's Bay Ni–Cu–Co sulfide deposit, Labrador, Canada. Mineralium Deposita, **47**(1–2): 23–50. doi:10.1007/s00126-011-0347-6.

Lister, J.R., and Kerr, R.C. 1991. Fluid-mechanical models of crack propagation and their application to magma transport in dykes. Journal of Geophysical Research, **96**(B6): 10,049–10,077.

Lodders, K. 2003. Solar system abundances and condensation temperatures of the elements. The Astrophysical Journal, **591**: 1220–1247. doi:10.1086/375492.

Lu, Y., Lesher, C.M., and Deng, J. 2019. Geochemistry and genesis of magmatic Ni–Cu–(PGE) and PGE–(Cu)–(Ni) deposits in China. Ore Geology Reviews, **107**: 863–887. doi:10.1016/j.oregeorev.2019.03.024.

Magee, C., Muirhead, J.D., Karvelas, A., Holford, S.P., Jackson, C.A.L., Bastow, I.D., Schofield, N., Stevenson, C.T.E., McLean, C., McCarthy, W., and Shtukert, O. 2016. Lateral magma flow in mafic sill complexes. Geosphere, **12**(3): 809–841. doi:10.1130/GES01256.1.

Maier, W.D., Li, C.S., and De Waal, S.A. 2001. Why are there no major Ni–Cu sulfide deposits in large layered mafic–ultramafic intrusions? The Canadian Mineralogist, **39**: 547–556. doi:10.2113/gscanmin.39.2.547.

Maier, W.D., Barnes, S.J., and Groves, D.I. 2013. The Bushveld Complex, South Africa: formation of platinum–palladium, chrome- and vanadium-rich layers via hydrodynamic sorting of a mobilized cumulate slurry in a large, relatively slowly cooling, subsiding magma chamber. Mineralium Deposita, **48**(1): 1–56. doi:10.1007/s00126-012-0436-1.

Maier, W.D., Howard, H.M., Smithies, R.H., Yang, S.H., Barnes, S.-J., et al. 2015. Magmatic ore deposits in mafic–ultramafic intrusions of the Giles Event, Western Australia. Ore Geology Reviews, **71**: 405–436.

Maier, W.D., Smithies, R.H., Spaggiari, C.V., Barnes, S.J., Kirkland, C.L., Yang, S., et al. 2016. Petrogenesis and Ni–Cu sulphide potential of mafic–ultramafic rocks in the Mesoproterozoic Fraser Zone within the Albany–Fraser Orogen, Western Australia. Precambrian Research, **281**: 27–46. doi:10.1016/j.precamres.2016.05.004.

Mainwaring, P.R., and Naldrett, A.J. 1977. Country rock assimilation and the genesis of Cu–Ni sulphides in the Waterhen intrusion, Duluth Complex, Minnesota. Economic Geology, **72**: 1269–1284.

Malich, N.S., Tazihin, N.N., Tuganova, E.V., Bunzen, E.A., Kulikova, N.G., and Safonova, I. 1974. Map of geological formations of the Siberian platform cover (1:1500 000).

Mao, J., Pirajno, F., Zhang, Z., Chai, F., Wu, H., Chen, S., et al. 2008. A review of the Cu–Ni sulphide deposits in the Chinese Tianshan and Altay orogens (Xinjiang Autonomous Region, NW China): principal characteristics and ore-forming processes. Journal of Asian Earth Sciences, **32**(2–4): 184–203. doi:10.1016/j.jseaes.2007.10.006.

Mao, Y.-J., Barnes, S.J., Duan, J., Qin, K.-Z., Godel, B.M., and Jiao, J. 2018. Morphology and particle size distribution of olivines and sulphides in the Jinchuan Ni–Cu sulphide deposit: evidence for sulphide percolation in a crystal mush. Journal of Petrology, **59**: 1701–1730. doi:10.1093/petrology/egy077.

Mariga, J., Ripley, E.M., and Li, C. 2006. Petrologic evolution of gneissic xenoliths in the Voisey's Bay Intrusion, Labrador, Canada: mineralogy, reactions, partial melting, and mechanisms of mass transfer. Geochemistry Geophysics Geosystems, **7**: Q0513. doi:10.1029/2005GC001184.

Mavrogenes, J.A., and O'Neill, H.S.C. 1999. The relative effects of pressure, temperature and oxygen fugacity on the solubility of sulfide in mafic magmas. Geochimica et Cosmochimica Acta, **63**: 1173–1180. doi:10.1016/S0016-7037(98)00289-0.

Menand, T. 2011. Physical controls and depth of emplacement of igneous bodies: a review. Tectonophysics, **500**(1–4): 11–19. doi:10.1016/j.tecto.2009.10.016.

Miller, J.D. 2011. Layered intrusions of the Duluth Complex. GSA Field Guide, **24**: 171–201. doi:10.1130/2011.0024(09).

Muirhead, J.D., Airoldi, G., White, J.D.L., and Rowland, J.V. 2014. Cracking the lid: sill-fed dikes are the likely feeders of flood basalt eruptions. Earth and Planetary Science Letters, **406**: 187–197. doi:10.1016/j.epsl.2014.08.036.

Mungall, J.E. 2007. Crustal contamination of picritic magmas during transport through dikes: the Expo Intrusive Suite, Cape Smith Fold Belt, New Quebec. Journal of Petrology, **48**(5): 1021–1039. doi:10.1093/petrology/egm009.

Mungall, J.E., and Brenan, J.M. 2003. Experimental evidence for the chalcophile behavior of the halogens. Canadian Mineralogist, **41**: 207–220. doi:10.2113/gscanmin.41.1.207.

Mungall, J.E., and Su, S. 2005. Interfacial tension between magmatic sulfide and silicate liquids: constraints on kinetics of sulfide liquation and sulfide migration through silicate rocks. Earth and Planetary Science Letters, **234**: 135–149. doi:10.1016/j.epsl.2005.02.035.

Mungall, J.E., Harvey, J.D., Balch, S.J., Atkinson, J., and Hamilton, M.A. 2010. Eagle's Nest: a magmatic Ni-sulfide deposit in the James Bay Lowlands, Ontario, Canada. Special Publication (Society of Economic Geologists (U.S.)), **15**: 539–557.

Mungall, J.E., Brenan, J.M., Godel, B., Barnes, S.J., and Gaillard, F. 2015. Transport of metals and sulphur in magmas by flotation of sulphide melt on vapour bubbles. Nature Geoscience, **8**(3): 216–219. doi:10.1038/NGEO2373.

Naldrett, A.J. 1966. The role of sulphurization in the genesis of iron – nickel sulphide deposits of the Porcupine district, Ontario. Canadian Institute of Mining and Metallurgy Transactions, **69**: 147–155.

Naldrett, A.J. 1992. A model for the Ni–Cu–PGE ores of the Noril'sk region and its application to other areas of flood basalt. Economic Geology, **87**(8): 1945–1962. doi:10.2113/gsecongeo.87.8.1945.

Naldrett, A.J. 2004. Magmatic sulfide deposits: geology, geochemistry and exploration. Springer, Heidelberg. 727 pp.

Naldrett, A.J. 2011. Fundamentals of magmatic sulfide deposits. Reviews in Economic Geology, **17**: 1–50.

Naldrett, A.J., Fedorenko, V.A., Lightfoot, P.C., Kunilov, V.I., Gorbachev, N.S., Doherty, W., and Johan, Z. 1995. Ni—Cu–PGE deposits of Noril'sk region, Siberia: their formation in conduits for flood basalt volcanism. Transactions of the Institution of Mining and Metallurgy, Section B: Applied Earth Science, **104**: B18–B36.

Nisbet, E.G., and Chinner, G.A. 1981. Controls on the eruption of mafic and ultramfic lava, Ruth Well Ni–Cu prospect, West Pilbara. Economic Geology, **76**: 1719–1735.

Nixon, G.T., Manor, M.J., Jackson-Brown, S., Scoates, J.S., and Ames, D.E. 2015. Magmatic Ni–Cu–PGE sulphide deposits at convergent margins. *In* Open File 7856. Geological Survey of Canada. pp. 17–34.

Paces, J.B., and Miller, J.D., Jr. 1993. Precise U–Pb ages of Duluth Complex and related mafic intrusions, northeastern Minnesota: geochronological insights to physical, petrogenetic, paleomagnetic, and tectonomagnetic processes associated with the 1.1 Ga Midcontinent Rift System. Journal of Geophysical Research, **98**(B8): 13997–14013. doi:10.1029/93JB01159.

Page, M.L., and Schmulian, M.L. 1981. The proximal volcanic environment of the Scotia nickel deposits. Economic Geology, **76**: 1469–1479. doi:10.2113/gsecongeo.76.6.1469.

Peck, D.C., Keays, R.R., James, R.S., Chubb, P.T., and Reeves, S.J. 2001. Controls on the formation of contact-type platinum-group element mineralization in the East Bull Lake intrusion. Economic Geology, **96**: 559–581. doi:10.2113/gsecongeo.96.3.559.

Perring, C.S. 2015. A 3-D geological and structural synthesis of the Leinster area of the Agnew–Wiluna belt, Yilgarn Craton, Western Australia, with special reference to the volcanological setting of komatiite-associated nickel sulfide deposits. Economic Geology, **110**(2): 469–503. doi:10.2113/econgeo.110.2.469.

Perring, C.S., Barnes, S.J., and Hill, R.E.T. 1995. The physical volcanology of komatiite sequences from Forrestania, southern Cross Province, Western Australia. Lithos, **34**: 189–207. doi:10.1016/0024-4937(95)90021-7.

Perring, C.S., Barnes, S.J., and Hill, R.E.T. 1996. Geochemistry of komatiites from Forrestania, southern Cross Province, Western Australia: evidence for crustal contamination. Lithos, **37**: 181–197. doi:10.1016/0024-4937(95)00036-4.

Polyakov, G.V., Tolstykh, N.D., Mekhonoshin, A.S., Izokh, A.E., Podlipskii, M.Y., Orsoev, D.A., et al. 2013. Ultramafic–mafic igneous complexes of the Precambrian East Siberian metallogenic province (southern framing of the Siberian craton): age, composition, origin, and ore potential. Russian Geology and Geophysics, **54**(11): 1319–1331. doi:10.1016/j.rgg.2013.10.008.

Porter, D.J., and McKay, K.G. 1981. The nickel sulfide mineralization and metamorphic setting of the Forrestania area, Western Australia. Economic Geology, **76**: 1524–1549. doi:10.2113/gsecongeo.76.6.1524.

Prendergast, M.D. 2003. The nickeliferous Late Archean Reliance komatiitic event in the Zimbabwe craton: magmatic architecture, physical volcanology, and ore genesis. Economic Geology, **98**: 865–891. doi:10.2113/gsecongeo.98.5.865.

Radko, V.A. 2016. The facies of intrusive and effusive magmatism in the Norilsk region. VSEGEI, St. Petersburg. 226 pp.

Ripley, E.M., and Al-Jassar, T.J. 1987. Sulfur and oxygen isotope studies of melt-country rock interaction, Babbitt Cu–Ni deposit, Duluth Complex, Minnesota. Economic Geology, **82**(1): 87–107. doi:10.2113/gsecongeo.82.1.87.

Ripley, E.M., and Li, C. 2013. Sulfide saturation in mafic magmas: is external sulfur required for magmatic Ni–Cu–(PGE) ore genesis? Economic Geology, **108**(1): 45–58. doi:10.2113/econgeo.108.1.45.

Ripley, E.M., Lightfoot, P.C., Li, C., and Elswick, E.R. 2003. Sulfur isotopic studies of continental flood basalts in the Noril'sk region: implications for the association between lavas and ore-bearing intrusions. Geochimica et Cosmochimica Acta, **67**(15): 2805–2817. doi:10.1016/S0016-7037(03)00102-9.

Ripley, E.M., Sarkar, A., and Li, C.S. 2006. Mineralogic and stable isotope studies of hydrothermal alteration at the Jinchuan Ni–Cu deposit, China. Economic Geology, **100**(7): 1349–1361. doi:10.2113/gsecongeo.100.7.1349.

Robertson, J., Ripley, E.M., Barnes, S.J., and Li, C. 2015*a*. Sulfur liberation from country rocks and incorporation in mafic magmas. Economic Geology, **110**(4): 1111–1123. doi:10.2113/econgeo.110.4.1111.

Robertson, J.C., Barnes, S.J., and Le Vaillant, M. 2015*b*. Dynamics of magmatic sulphide droplets during transport in silicate melts and implications for magmatic sulphide ore formation. Journal of Petrology, **56**(12): 2445–2472. doi:10.1093/petrology/egv078.

Samalens, N., Barnes, S.J., and Sawyer, E.W. 2017. The role of black shales as a source of sulfur and semimetals in magmatic nickel–copper deposits: example from the Partridge River Intrusion, Duluth Complex, Minnesota, USA. Ore Geology Reviews, **81**(Part 1): 173–187. doi:10.1016/j.oregeorev.2016.09.030.

Saumur, B.M., Cruden, A.R., and Boutelier, D. 2015. Sulfide liquid entrainment by silicate magma: implications for the dynamics and petrogenesis of magmatic sulfide deposits. Journal of Petrology, **56**(12): 2473–2490. doi:10.1093/petrology/egv080.

Schmidt, J.M., and Rogers, R.K. 2007. Metallogeny of the Nikolai large igneous province (LIP) in southern Alaska and its influence on the mineral potential of the Talkeetna Mountains. *In* Tectonic growth of a collisional continental margin: crustal evolution of southern Alaska. Special Paper 431. *Edited by* K.D. Ridgway, J.M. Trop, J.M.G. Glen, and J.M. O'Neill. Geological Society of America. pp. 623–648.

Scoates, J.S., and Mitchell, J.N. 2000. Evolution of troctolitic and high Al basaltic magmas in Proterozoic anorthosite plutonic suites and implications for the Voisey's Bay massive Ni–Cu sulfide deposit. Economic Geology, **95**(4): 677–701. doi:10.2113/gsecongeo.95.4.677.

Seat, Z., Beresford, S.W., Grguric, B.A., Waugh, R.S., Hronsky, J.M.A., Gee, M.A.M., Groves, D.I., and Mathison, C.I. 2007. Architecture and emplacement of the Nebo-Babel gabbronorite-hosted magmatic Ni–Cu–PGE sulphide deposit, West Musgrave, Western Australia. Mineralium Deposita, **42**(6): 551–581. doi:10.1007/s00126-007-0123-9.

Self, S., Schmidt, A., and Mather, T.A. 2014. Emplacement characteristics, time scales, and volcanic gas release rates of continental flood basalt eruptions on Earth. Geological Society of America Special Papers, **505**: 319–337. doi:10.1130/2014.2505(16).

Smythe, D.J., Wood, B.J., and Kiseeva, E.S. 2017. The S content of silicate melts at sulfide saturation: new experiments and a model incorporating the effects of sulfide composition. American Mineralogist, **102**(4): 795–803. doi:10.2138/am-2017-5800CCBY.

Song, X.-Y., Zhou, M.-F., Keays, R.R., Cao, Z.-M., Sun, M., and Qi, L. 2006. Geochemistry of the Emeishan flood basalts at Yangliuping, Sichuan, SW China: implications for sulfide segregation. Contributions to Mineralogy and Petrology, **152**(1): 53–74. doi:10.1007/s00410-006-0094-3.

Song, X., Zhou, M., Tao, Y., and Xiao, J. 2008. Controls on the metal compositions of magmatic sulfide deposits in the Emeishan large igneous province, SW China. Chemical Geology, **253**(1–2): 38–49. doi:10.1016/j.chemgeo.2008.04.005.

Song, X., Keays, R.R., Xiao, L., Qi, H., and Ihlenfeld, C. 2009*a*. Platinum-group element geochemistry of the continental flood basalts in the central Emeishan large igneous province, SW China. Chemical Geology, **262**(3–4): 246–261. doi:10.1016/j.chemgeo.2009.01.021.

Song, X.Y., Keays, R.R., Zhou, M.F., Qi, L., IhIenfeld, C., and Xiao, J.F. 2009*b*.

Siderophile and chalcophile elemental constraints on the origin of the Jinchuan Ni–Cu–(PGE) sulfide deposit, NW China. Geochimica et Cosmochimica Acta, **73**(2): 404–424. doi:10.1016/j.gca.2008.10.029.

Song, X., Danyushevsky, L.V., Keays, R.R., Chen, L., Wang, Y., Tian, Y., et al. 2012. Structural, lithological, and geochemical constraints on the dynamic magma plumbing system of the Jinchuan Ni–Cu sulfide deposit, NW China. Mineralium Deposita, **47**(3): 277–297. doi:10.1007/s00126-011-0370-7.

Sproule, R.A., Lesher, C.M., Ayer, J.A., Thurston, P.C., and Herzberg, C.T. 2002. Spatial and temporal variations in the geochemistry of komatiites and komatiitic basalts in the Abitibi greenstone belt. Precambrian Research, **115**: 153–186. doi:10.1016/S0301-9268(02)00009-8.

Sproule, R.A., Lesher, C.M., Sutcliffe, R., and Tracanelli, H. 2005. Nipissing-aged Ni–Cu–PGE mineralization in the Shakespeare intrusion. Applied Earth Science (Trans. Inst. Min. Metall. B), **116**(4): 239–242.

Staude, S., Barnes, S.J., and Le Vaillant, M. 2017. Thermomechanical erosion of ore-hosting embayments beneath komatiite lava channels: textural evidence from Kambalda, Western Australia. **90**: 446–464. doi:10.1016/j.oregeorev.2017.05.001.

Stone, W.E., Crocket, J.H., and Fleet, M.E. 1996. Platinum-group mineral occurrence associated with flow top amygdule sulfides in komatiitic basalt, Abitibi Greenstone Belt, Ontario. Mineralogy and Petrology, **56**(1–2): 1–24. doi:10.1007/BF01162655.

Su, S., Mungall, J., Wang, J., and Geng, K. 2005. Interfacial tension studies between Fe–Cu–Ni sulfide and halo-Norilsk basalt slag system. Science in China Series D, Earth Sciences, **48**(6): 834–839. doi:10.1360/03yd0023.

Svensen, H.H., Torsvik, T.H., Callegaro, S., Augland, L., Heimdal, T.H., Jerram, D.A., Planke, S., and Pereira, E. 2018. Gondwana Large Igneous Provinces: plate reconstructions, volcanic basins and sill volumes. Geological Society, London, Special Publications, **463**(1): 17. doi:10.1144/SP463.7.

Tang, Z. 1993. Genetic model of the Jinchuan nickel–copper deposit. Geological Association of Canada Special Paper, **40**: 389–401.

Taranovic, V., Ripley, E.M., Li, C., and Rossell, D. 2015. Petrogenesis of the Ni—Cu–PGE sulfide-bearing Tamarack intrusive complex, Midcontinent Rift System, Minnesota. Lithos, (Oslo) **212–215**: 16–31. doi:10.1016/j.lithos.2014.10.012.

Thomson, K. 2007. Determining magma flow in sills, dykes and laccoliths and their implications for sill emplacement mechanisms. Bulletin of Volcanology, **70**(2): 183–201. doi:10.1007/s00445-007-0131-8.

Tonnelier, N. 2010. Geology and genesis of the Jinchuan Ni–Cu–(PGE) deposit, China. Department of Earth Sciences, Laurentian University, Sudbury, Ont. 261 pp.

Tonnelier, N., Lesher, C.M., and Arndt, N.T. 2013. Source controls on the metal contents of mantle-derived magmas. Mineralogical Magazine, **77**(5): 2344. doi:10.1180/minmag.2013.077.5.20.

Townsend, M., Pollard, D., and Smith, R. 2017. Mechanical models for dikes: a third school of thought. Tectonophysics, **703**: 98–118. doi:10.1016/j.tecto.2017.03.008.

Ullmann, A., Zamir, M., Ludmer, Z., and Brauner, N. 2003. Stratified laminar countercurrent flow of two liquid phases in inclined tubes. International Journal of Multiphase Flow, **29**(10): 1583–1604. doi:10.1016/S0301-9322(03)00144-7.

Viljoen, M.J., Bernasconi, A., van Coller, N., Kinloch, E., and Viljoen, R.P. 1976. The geology of the Shangani nickel deposit, Rhodesia. Economic Geology, **71**: 76–95. doi:10.2113/gsecongeo.71.1.76.

Wang, C.Y., Wei, B., Zhou, M.-F., Minh, D.H., and Qi, L. 2018. A synthesis of magmatic Ni—Cu–(PGE) sulfide deposits in the ~260 Ma Emeishan large igneous province, SW China and northern Vietnam. **154**: 162–186. doi:10.1016/j.jseaes.2017.12.024.

Wendlandt, R.F. 1982. Sulfide saturation of basalt and andesite melts at high pressure. American Mineralogist, **67**: 877–885.

White, S.M., Crisp, J.A., and Spera, F.J. 2006. Long-term volumetric eruption rates and magma budgets. Geochemistry, Geophysics, Geosystems, **7**(3): Q03010. doi:10.1029/2005GC001002.

Williams, D.A., Kerr, R.C., and Lesher, C.M. 1998. Emplacement and erosion by Archean komatiite lava flows at Kambalda: revisited. Journal of Geophysical Research: Solid Earth, **103**: 27533–27549. doi:10.1029/97JB03538.

Williams, D.A., Kerr, R.C., Lesher, C.M., and Barnes, S.J. 2001. Analytical/numerical modeling of komatiite lava emplacement and thermal erosion at Perseverance, Western Australia. Journal of Volcanology and Geothermal Research, **110**: 27–55. doi:10.1016/S0377-0273(01)00206-2.

Williams, D.A., Kadel, S.D., Greeley, R., Lesher, C.M., and Clynne, M.A. 2004. Erosion by flowing lava: geochemical evidence in the Cave Basalt, Mount St. Helens, Washington. Bulletin of Volcanology, **66**(2): 168–181. doi:10.1007/s00445-003-0301-2.

Williams, D.A., Kerr, R.C., and Lesher, C.M. 2011. Mathematical modeling of thermomechanical erosion beneath Proterozoic komatiitic basaltic sinuous rilles in the Cape Smith belt, New Québec, Canada. Mineralium Deposita, **46**(8): 943–958. doi:10.1007/s00126-011-0364-5.

Wilson, A.H. 2012. A chill sequence to the Bushveld Complex: insight into the first stage of emplacement and implications for the parental magmas. Journal of Petrology, **53**(6): 1123–1168. doi:10.1093/petrology/egs011.

Wilson, L., and Head, J.W. 1981. Ascent and eruption of basaltic magma on the earth and moon. Journal of Geophysical Research: Solid Earth, **86**: 2971–3001. doi:10.1029/JB086iB04p02971.

Wingate, M.T.D., Pirajno, F., and Morris, P.A. 2004. Warakurna Large Igneous Province: a new Mesoproterozoic large igneous province in west-central Australia. Geology, **32**(2): 105–108. doi:10.1130/G20171.1.

Young, S.A., Loukola-Ruskeeniemi, K., and Pratt, L.M. 2013. Reactions of hydrothermal solutions with organic matter in Paleoproterozoic black shales at Talvivaara, Finland: evidence from multiple sulfur isotopes. Earth and Planetary Science Letters, **367**: 1–14. doi:10.1016/j.epsl.2013.02.004.

Zhang, M., O'Reilly, S.Y., Wang, K.-L., Hronsky, J., and Griffin, W. 2008. Flood basalts and metallogeny: the lithosphere mantle connection. Earth Science Reviews, **86**: 145–174.

Zhou, M.F., Kennedy, A.K., Sun, M., Malpas, J., and Lesher, C.M. 2002. Neoproterozoic arc-related mafic intrusions along the northern margin of South China: implications for the accretion of Rodinia. Journal of Geology, **110**(5): 611–618. doi:10.1086/341762.

Zhu, L., Jin, N.-D., Gao, Z.-K., and Zong, Y.-B. 2011. Multi-scale cross entropy analysis for inclined oil–water two-phase countercurrent flow patterns. Chemical Engineering Science, **66**(23): 6099–6108. doi:10.1016/j.ces.2011.08.034.

Zhu, L., Jin, N., Gao, Z., and Zong, Y. 2014. Multifractal analysis of inclined oil–water countercurrent flow. Petroleum Science, **11**(1): 111–121. doi:10.1007/s12182-014-0322-9.

Zong, Y.-B., Jin, N.-D., Wang, Z.-Y., Gao, Z.-K., and Wang, C. 2010. Nonlinear dynamic analysis of large diameter inclined oil–water two phase flow pattern. International Journal of Multiphase Flow, **36**(3): 166–183. doi:10.1016/j.ijmultiphaseflow.2009.11.006.

Zotov, I.A. 1976. Some characteristics of the reaction of trap magmas of the Talnakh intrusions (Norilsk area) with surrounding rocks. *In* Ocherki geologicheskoy petrologii. *Edited by* O.A. Bogatikov, A.M. Borsuk, and A.K. Simon. Izd. Nauka, Moscow, USSR. pp. 250–260.